RADIATIVE TRANSFER IN CIRCUMSTELLAR DUST

By

CHRISTOPHER ALVIN HARVEL

A DISSERTATION PRESENTED TO THE GRADUATE COUNCIL OF
THE UNIVERSITY OF FLORIDA
IN PARTIAL FULFILLMENT OF THE REQUIREMENTS FOR THE
DEGREE OF DOCTOR OF PHILOSOPHY

UNIVERSITY OF FLORIDA

1974

to my parents

ACKNOWLEDGMENTS

I would like to thank Professor Sabatino Sofia for suggesting this problem to me and for the inspiration and guidance he has given me toward a solution. I would also like to thank Professors Frank Bradshaw Wood, Kwan-Yu Chen, Howard L. Cohen, and James W. Dufty for serving on my committee.

I have enjoyed, greatly appreciated, and profited by many valuable discussions with Andy Endal, Wayne McClain, Joe Mullen, Liz Mullen, Al Rust, and Wilbur Schneider.

The curve plotting done by Andy Endal, the drafting done by Charley Bottoms and Joe Mullen, and the typing of the entire manuscript done by Nadia Scheffer are also greatly appreciated.

Computing time for the project was donated by the Northeast Regional Data Center of the University of Florida and the Central Florida Regional Data Center of the University of South Florida.

TABLE OF CONTENTS

Abstract of Dissertation Presented to the Graduate Council of the University of Florida in Partial Fulfillment of the Requirements for the Degree of Doctor of Philosophy

RADIATIVE TRANSFER IN CIRCUMSTELLAR DUST

By

Christopher Alvin Harvel

August, 1974

Chairman: Frank Bradshaw Wood
Major Department: Astronomy

A procedure is developed to calculate the radiation field as a function of position, direction, and wavelength within a spherically symmetric circumstellar dust shell. The dust shell is assumed to consist of grey isotropically scattering dust particles in thermal equilibrium with the radiation field and to be characterized by seven parameters--(1) the radius of the central star, (2) the inner radius of the shell, (3) the outer radius of the shell, (4) the total optical depth of the shell, (5) an index which specifies the density distribution, (6) the albedo of the dust particles, and (7) the temperature of the central star.

The temperature distribution and the radiation field within several model dust shells are determined, and used to calculate for each shell the spectral-energy distribution of the radiation emitted. These models are compared to those of other authors. It is found that fitting the visual spectral-energy distribution of an observed object does not necessarily mean that the model parameters so obtained are

consistent with the infrared part of the objects' spectral energy distribution, and that the shape of the spectral energy distribution can be strongly dependent on the index in the assumed power law density distribution.

The procedure is applied to the two infrared objects--HD 45677 and R Monocerotis.

SECTION I
INTRODUCTION

This paper will consider the problem of radiative transfer in a spherical shell of dust particles illuminated by a central star. In such a shell a dust particle will absorb, reemit and scatter the radiation from both the central star and the other particles of the shell. Since the star will, in general, be much hotter than the particles, the radiation field will consist of a visual part, due primarily to the star and an infrared part due primarily to the dust. Therefore, the solution of the transfer problem must take into account absorption, reemission and scattering of both these parts of the radiation field.

The solution of this transfer problem will yield the quantities which characterize the radiation field at any point in the shell and at any frequency - the intensity and the flux for example. Using these quantities we can describe the flow of energy from the star to the outer edge of the shell and predict the observational characteristics of the shell. Also, from a theoretical point of view the radiation field within the dust shell is of considerable interest, since it determines a number of physical quantities related to the matter in the shell. The temperature of the dust particles, the radiation pressure on the dust

and gas and the excitation and ionization states of the gas are all dependent on the radiation field.

From a knowledge of the dust temperature within the shell we can limit the number of possible materials of which the dust particles can be composed. According to Gilman (1969), at temperatures above 1500°K, refractory silicates such as Al_2SiO_5 will be the most important condensates around oxygen-rich stars while carbon will dominate around carbon-rich stars - below this temperature a number of other compounds can begin to condense. A knowledge of the radiation pressure as a function of distance from the star will allow us to compare its effect on the material there with that of other forces such as the gravitational force and the force due to high velocity particles which might be ejected from the central star. The ionization and excitation state of the gas associated with a dust shell can be of considerable importance in calculating models for collapsing, rotating photostars interacting with an external magnetic field (Prentice and ter Haar, 1971).

The observational characteristics of the shell which the solution of the transfer problem would yield are of considerable interest because of the recent availability of a great deal of observational information at infrared wavelengths. In the past few years a large number of objects have been discovered which emit more infrared radiation than expected. Many of these infrared objects emit most of their radiation in the region to the red of 1μ and have

gone undetected in the past because of the low sensitivity of detectors in that region. Since 1965 the region between 1 and 20μ has been surveyed extensively and several thousand infrared sources have been discovered. A partial list of these surveys follows: the California Institute of Technology survey at 2.2μ which discovered approximately 5600 sources (Neugebauer and Leighton, 1969), surveys for red stars using IN plates by Hetzler (1937), Chavira (1967), Ackermann et al. (1968), and Ackermann (1970), and surveys at wavelengths longer than 10μ (e.g., Low 1970).

Many of the objects discovered in these surveys have an excess of radiation within a given infrared wavelength interval, as compared with a black-body with an effective temperature appropriate to the objects observed spectral type. This excess of infrared radiation is usually referred to as an "infrared excess." Most of the 5600 objects discovered in the 2.2μ survey have been identified with late-type giant stars (Grasdalen and Gaustad, 1971) but about 50 of the reddest of these objects could not be identified with cataloged visual sources. These very red sources are manifestations of a wide variety of physical objects, including according to Neugebauer et al. (1971), HII regions, planetary nebulae, M supergiant stars, late-type giant stars, RV Tauri stars, novae, Be stars, and T Tauri stars and related objects. Most of the infrared excesses associated with the T Tauri stars and related objects are assumed to result from thermal radiation from a circumstellar

dust shell. This assumption is also made for Be stars but in their case it has been argued by some authors, e.g. Woolf et al. (1970), that the observed infrared emission is consistent with free-free emission from ionized hydrogen. For those objects other than the Be stars and the T Tauri stars and related objects thermal radiation by dust is probably present but may not be the principal cause of the observed infrared excess.

Since a general solution of the transfer problem for circumstellar dust shells would be readily applicable to the T Tauri stars and related objects a more detailed description of these objects will be given at this point.

The T Tauri stars and related objects form an especially interesting group from both an observational and a theoretical point of view. Poveda (1965a) pointed out in 1965 that T Tauri stars, which for the last 20 years have been assumed to be young gravitationally contracting objects, might have thick circumstellar dust shells. He argued that such a shell would be a remnant of the contracting cloud from which the star formed and that it would be bright in the infrared. Shortly after this Mendoza (1966) found that most T Tauri stars do have infrared excesses and later Mendoza (1968) found that the bolometric luminosity of these objects was from 1.3 to 6.6 times that expected from the visual observations. For R Monocerotis, an object closely related to the T Tauri stars, Mendoza (1968) found the bolometric luminosity to be 58 times that expected from the

visual data. Figure 9 shows the spectral-energy distribution of R Monocerotis and it can be seen that most of the observed luminosity is emitted beyond 1μ.

The T Tauri stars are Hα emission stars, and in the early 1940's all such emission stars were studied spectroscopically because of the intrinsic value of their spectra. It was not until 1945 that Joy (1945) recognized T Tauri stars as a distinct class of emission-line variables associated with nebulosity.

From a study of eleven stars, Joy established the criterion to be used in assigning stars to this new class. He describes in detail each of the eleven stars and says that the spectra in general are F5-G5, but that there is a small variation in spectral type with the brightness. Also, absorption lines are usually lacking but many bright lines of low excitation are present. He points out the similarity between the spectra of these stars and the solar chromosphere. For five of the stars he finds color excesses, which he attributes to strong selective absorption of the nebulosity. He finds that usually the emission lines seen are displaced to the violet of the absorption lines (if any absorption lines are present), and that it is very difficult to say anymore about the radial velocities of these stars.

In a review article on T Tauri stars and related objects, Herbig (1960) points out that the only conclusive test for membership in the T Tauri class is provided by the spectroscopic data.

The classification system in use today is described in and employed by the Third Edition of The General Catalogue of Variable Stars (Kukarkin et al., 1969). The criteria given in the catalogue are those adopted by the IAU Commission 27. These criteria are spectroscopic with one exception, which is, that if the variable is connected with diffuse nebulae it is designated InT whereas if it is not it is designated IT. The prototype is stated to be T Tauri.

The catalogue breaks the irregular nebular variables into several classes, one of which, InT, represents the T Tauri stars. Its class Is is the same as Hoffmeister's RW Aur class, and differs little from the InT class. Three more of the classes defined by the catalogue, In, Ins, and Inb, contain young objects of spectral class F-M with irregular light variations (these have been called the Orion variables). Of its nebular variable class the catalogue class Ina (early spectral type Orion variables) differs the most from class InT.

In some of the current literature stars falling into all these classes are referred to as T Tauri stars and related objects, although usually only in the sense that the star is in an early evolutionary stage can it be grouped with the T Tauri variables.

R Mon, the unusual object observed by Mendoza, is not included in class InT because it is assigned by a Russian author to spectral class A-Fep, which is too early a spectral class for an InT variable. Joy (1945) originally

classified it as approximately G, and Mendoza (1968) classifies it as K. Thus this star has been assigned spectral classifications from A through K. This points out an important fact; namely, the spectral classification of T Tauri stars is very difficult because of the lack of a strong absorption spectrum.

Most of these stars are rather faint; the brightest of the class is about $m_v = +9$ at maximum light. The magnitude usually quoted for T Tauri variables is the mean of the observed magnitude, even though this may not be the most meaningful value.

For the last twenty years T Tauri stars have been assumed to be pre-main-sequence (PMS) stars and recently PMS models have become available which might help to verify this assumption. The best proto-star models at present are those of Hayashi (1966) and Larson (1969b). Both of these models are directly applicable to the problem of the T Tauri phenomena.

For his model Larson assumes that the initial proto-stellar cloud is spherical, not rotating, and free of magnetic fields. He does not assume, as Hayashi does, that the collapse is homologous and that the density follows a polytropic law. Initially the cloud has the Jeans radius ($R = v_s[G\rho]^{-1/2}$, where v_s = the velocity of sound, G = the gravitational constant, ρ = the density), and a density of 1.10×10^{-19} gm/cm^3. The time scale for collapse in this model goes as $1/\sqrt{\rho}$, so that the density gradient increases

with time, resulting in a dense core, which finally gains the size and mass of a star. The core then evolves toward the Main Sequence (MS) while accreting matter from the lower density cloud about it.

If the mass of the cloud is $2.5M_{\odot}$ or less, the proto-star will become visible somewhere along the lower part of the fully convective Hayashi track; if it is somewhat more massive it becomes visible at some point on the radiative track running horizontally toward the MS; if it is very massive (as massive as an O or B MS star) it does not become visible until reaching the MS.

The time required in Larson's model for the accretion of the envelope depends on the mass of the proto-star, and ranges from 10^5 to 10^6 years.

Hayashi's computations start with a proto-star of much higher density, and in his model the accretion of the cloud, which brings the proto-star to the beginning of the fully convective phase, takes place in a few decades.

The two models differ in their treatment of the shock phenomena at the interface between the shell and the dense core, but the latter parts of their evolutionary tracks are in agreement. In both models we have a dense core and a circumstellar shell, and Strom (1972) points out that we should expect some young stellar objects to show evidence of the remnants of their shells. These proto-star models neither explain nor predict the variability, line emission, and mass ejection observed for the T Tauri stars.

There are a number of reasons for believing that the T Tauri stars are PMS objects: (1) their large red and infrared excesses and deficiencies; (2) their position on the H-R diagram (above and below the MS); (3) their association with dense interstellar matter; (4) their association with O and B stars; (5) their apparent rotational velocities; (6) their anomalous Li abundance; (7) their polarization.

As noted earlier, Joy (1945) found that almost half of his T Tauri stars had color excesses. Since then other authors have found large infrared excesses for some stars, and infrared deficiencies for others.

Mendoza (1966) did photometry in the UBVRIJKLM bands from .36μ to 5μ for 26 stars, including T Tauri, RW Aur, R Mon and Lk Hα 120. His observations show red excesses for most of the stars, a deficiency (E_{V-R} - 0.2) for DF Tau most likely caused by the Hα line in emission in the V band, and infrared excesses (from 0.9 to 5μ) for all the stars (E_{V-M} = 8.5 for R Mon).

Two years later Mendoza (1968) published another set of photometric observations on Johnson's nine color system; this time for 33 stars, some of which he had observed previously (Mendoza, 1966). His results were similar to those of 1966. He states that the two stars with the largest infrared excesses are R Mon and R CrA. Most of the objects observed by Mendoza (1966, 1968) were T Tauri stars.

In making the observations described above Mendoza used the 60" infrared telescope at the Catalina observatory

in Arizona. He notes that making observations of these objects is made difficult by their faintness and their close association with nebulosity. He tried various diaphram sizes from 36 to 13 seconds of arc in diameter, and found that in many cases a diaphram smaller than 13 seconds was actually needed.

From his observed fluxes, Mendoza (1968) computes bolometric corrections, and then absolute magnitudes for several of these objects. He finds that they have high luminosities, and speculates that Joy (1945) classified them as dwarfs because of their rather wide absorption lines.

To explain his 1966 observations Mendoza (1966) advanced two theories: (1) a multiple star system in which one of the components is a very cool infrared star, and (2) a core-envelope model in which the UBV photometry pertains to the core and the infrared photometry to the envelope. In this paper (Mendoza, 1966) he does not favor one theory over the other.

In the second paper Mendoza (1968) states that his previous core-envelope model is probably the explanation for the large infrared excesses observed for objects such as R Mon and R CrA. For the objects with small infrared excesses (infrared just a few times the visual) he suggests that the cause is heating of the stellar wind by cosmic rays.

He points out that his observations indicate that the envelope around the core behaves like a neutral filter in the visual (UBV) region. Assuming that all the infrared

radiation comes from this envelope, he finds that it would have a radius of about 10 AU and a mass of about 10^{-3} $M_{\odot}$.

Low and Smith (1966) published the results of their photometry of R Mon at 20μ. They found that at that wavelength the star was about one fourth as bright as Mondoza (1966) found it to be at 3.4μ.

To explain their observations they computed the spectral-energy-distribution to be expected from an optically thin circumstellar dust shell in which scattering and reabsorption of infrared radiation emitted by the dust can be neglected. The theoretical distribution they obtained matched the available observations fairly well.

Strom et al. (1972) observed 42 stars in NGC 2264 at 1.6, 2.2, and 3.4μ,and found infrared excesses and some infrared deficiencies. The authors state that these observations are an indication that the stars have circumstellar shells. They used profiles of the observed hydrogen lines to estimate the surface gravities of some of the PMS A stars in their sample of 42 NGC 2264 stars. From these surface gravities they computed luminosities, and found that those stars that seemed the faintest, as compared with their computed luminosities, all had infrared excesses. They suggest that these infrared excesses are due to a dust shell, radiating in the infrared, energy it has absorbed from the star in the visual part of the spectrum. The stars that they found to have the largest infrared excesses, were those that lie below the MS.

Strom et al. (1972) also found that these shells have a very high ratio of total to selective absorption, which would suggest large dust particles. The dust shells of lowest temperature were around the latest stars.

They speculate that the infrared deficiencies observed could be due to a very cool dust shell at a great distance from the central star. Of course, observations in the far infrared should find the missing radiation.

Martin Cohen (1973b) has observed stars in NGC 2264, IC 5146, VI Cyg and NGC 7000 (The North American Nebulae). NGC 7000 contains the T Tauri star Lk Hα 190, which was discovered by Herbig in 1958, and has recently brightened visually by 6 magnitudes.

Cohen used the 60" Catalina infrared telescope, and made observations in all wavelengths in a single night (this is very important since these objects vary rapidly). He concluded that for most of these stars (many of them not T Tauri stars) thermal emission from circumstellar dust is the cause of the infrared excesses he observed. In a few cases, he says that free-free emission from a circumstellar shell may be important out to about 11μ .

Breger (1972), like Cohen, finds evidence for circumstellar shells about PMS stars in NGC 2264. As well as infrared excesses, he finds light variability, which he attributes to circumstellar shells.

Strom et al. (1971) found a small amount of continuous and Hα emission, similar to that found for T Tauri stars, in

the spectra of some A-F stars in young clusters. They attribute this to very thin circumstellar shells. They also say that the strength of these features increases as the circumstellar absorption does.

According to Strom (1972) we should expect to see free-free (electron-H ion) and free-bound emission from envelopes in the infrared, if they have sufficient size and density. Dust envelopes, as stated previously, would show thermal infrared reradiation; thus, Strom (1972) ascribes the circumstellar emission in the optical region of T Tauri spectra to gas (this is the emission that washes out the normal absorption spectrum). He says that, in a joint paper, Kuhi and the Stroms indicate that gas shell emission may also dominate the infrared region.

In support of his idea that gas and not dust shell emission is dominant in the infrared, Strom (1972) offers the following argument and observational evidence. He finds that for some young stars (especially A-F stars) with circumstellar shells, Hα emission and infrared excesses there exists a correlation between log (Hα intensity) and the L magnitude (3.4μ). In an optically thin case of the dust model the dust emission is proportional to the optical depth ($\tau = \rho \times \text{length}$), whereas the gas emission (Hα) depends on $\rho^2 \times \text{length}$. Therefore, unless we believe that all circumstellar shells have the same densities, the dust theory is difficult to defend, because we would not get the observed correlation.

According to Herbig, in the Taurus cloud, Orion nebulae, NGC 2264, NGC 6530, and IC 5146, we find that if we fit the brightest T Tauri stars to a MS with a distance modulus of 6 the M1 to M3 stars observed are too bright. Thus, the observed MS in these regions appears to be turned up on the red end; however, the observed MS does not curve upward more and more as we observe later and later stars, but runs parallel to the Zero Age Main Sequence (ZAMS) after sharply breaking off from it at about A0. This observed MS forms a band with its upper edge several magnitudes above the ZAMS.

Herbig (1960) believes that the uncertainties in the observations and theory are large enough so that we need not be concerned by the fact that the observed MS does not curve upward. He also believes that part of the spread in the observed lower MS is caused by a spread in the times of stellar formation in the cluster.

Hayashi's evolutionary tracks for proto-stars would lead us to expect young stars to lie above the ZAMS.

Poveda (1965a) first brought attention to objects falling below the ZAMS in NGC 2264. He said that their location below the ZAMS was caused by thick circumstellar dust shells.

Strom et al. (1972), as we have seen, were able to show that those stars, in NGC 2264, lying below the MS would be above it, if their circumstellar shells were removed.

Presumably, the stars below the MS are younger than those above it, and have not had time to flatten their

circumstellar shells. According to Mendoza (1968), the T Tauri stars with the least infrared excess are the oldest, and have the most flattened disk-like shells. If we are looking at a disk edge on, we should see a large discrepancy between the luminosity as determined from the spectral classification, and the bolometric luminosity observed. Strom (1972) finds, for a sample of 10 Herbig Ae and Be stars, that for three, $L_{sp} >> L_{bolometric}$.

According to Strom et al. (1972), the presence of late-type stars near the MS in young clusters is caused by circumstellar obscuration, and not by a large spread (several x 10^7 years) in times of stellar formation, as argued by Herbig (1960).

T Tauri stars are found directly associated with the clouds in which they presumably formed. They can not be interlopers from the general field around the region in which they are found, since their space density averages 1 or 2 orders of magnitude above that of the field stars of the same luminosity (Herbig, 1960).

Cohen (1973c) has observed the T Tauri type objects at the tips of several cometary nebulae. Mendoza (1966) states that T Tauri and R Mon illuminate bright nebulosities. Both of these nebulosities are variable cometary nebulae. R Mon is in NGC 2261, Hubbles variable nebulae, and T Tauri is in NGC 1555, Hind's nebulae.

Poveda (1965c) describes the cometary nebulae (elephant trunks, bright rims, etc.) as HII regions expand-

ing into a surrounding HI region, or as a HII region expanding past an area of high density, compressing and deforming it. If either of these explanations is correct, the tip of such a nebulae will be a region of high density, suitable for star formation. Thus, cometary nebulae are very young phenomenon illuminated by even younger stars.

If we assume the stars have the space velocities of the eddy of gases from which they formed (about 2 km/sec), and if we estimate the size in km of the tip of the nebulae, we can estimate how long it would take the star to drift out of the tip, and thereby arrive at an upper estimate for the age of the star. Poveda does this for several nebulae, and finds ages running from 5×10^3 to 50×10^3 years.

Mendoza (1968) also makes a calculation to obtain the ages of some T Tauri stars. He uses the PMS evolutionary tracks of Iben to determine the age of a star from its position on the H-R diagram. The ages Mendoza obtains in this way agree with those of Poveda for some stars and disagree for others.

For R Mon the two methods agree rather well, but for the other stars Poveda's results are, in general, lower than Mendoza's.

Herbig (1960) states that in regions such as Orion, we find T Tauri stars associated with O and B stars, which are considered to be young objects. It seems logical then, to consider the T Tauri stars to be of similar age (hence young), but of lower mass, and thus not as greatly evolved.

Joy (1945) classified the T Tauri stars as MS dwarfs, which we now know to be incorrect. Those T Tauri stars that do show absorption lines, have very wide lines, which might indicate that they were luminosity class V objects. However, it is now believed that these abnormally wide absorption lines are caused by rotational broadening (Herbig, 1960).

The rotational velocities found for these stars (20 km.sec < v sin i < 65 km/sec) are unsually high for stars of their spectral class. Normal G-K stars have v sin i < 15 km/sec.

If we compute the radii of the T Tauri stars from their observed luminosity and color-temperature, and then assume they contract without loss of angular momentum along a Hayashi track, we can find their rotational velocities on the MS. When this is done, the computed values are in close agreement with observed values of v sin i for MS stars of comparable mass. It may of course be true that the line broadening is not caused by rotation.

The T Tauri stars as a group appear to be overabundant in Li, as compared with the Sun, by 1 or 2 orders of magnitude, which is taken as an indication of their youth (Herbig, 1960). Herbig compared the Li abundance of the T Tauri stars to that of chondritic meteorites, which presumably have the Li abundance of the pre-solar nebulae.

It is possible that the large abundance of Li is being caused by Li production in the photospheric layers of the T

Tauri stars, in which case it may not be an indication of their youth. It seems unlikely though that such Li production is actually occuring, since the most plausible mechanisms suggested for Li production require large, strong magnetic fields, which have not been observed.

Zellner (1970), Capps and Dyck (1972) and Breger and Dyck (1972) observe polarization for some stars in the near and far infrared. Zellner's measurements for R Mon indicate polarization typical of large grains (radius $\sim$ 0.1μ) while the other authors cited indicate that their measurements favor electron scattering similar to that observed for Be stars. In a more recent paper Zellner and Serkowski (1972) state that R CrA exhibits polarization similar to R Mon. They suggest that in objects such as R Mon and R CrA the dust cloud producing the infrared excess is in the form of an equatorial disk and the light seen at shorter wavelengths is scattered light which has filtered out the poles of this disk.

Breger and Dyck find that between 3000 and 7500 Å, four out of a sample of 35 stars in NGC 2264 show intrinsic polarization. Most of the stars they observed were not T Tauri stars, but of the four showing polarization one is a T Tauri star. Breger and Dyck comment that its polarization has a different λ dependence from that they observe for the other three polarized stars in their sample, and that its polarization is also different from that of T Tauri, as given by Serkowski (1971).

These investigations indicated the presence of circumstellar shells about T Tauri stars and stars in clusters associated with T Tauri stars, such as NGC 2264.

Some other important characteristics exhibited by young stars and T Tauri stars are the following: (1) mass loss and the P Cyg effect, (2) mass accretion and the inverse P Cyg effect, (3) ultraviolet excess, and (4) correlations of the visual magnitude and the infrared emission, of the Hα UV and IR emissions, and between mass infall and the V magnitude.

Most T Tauri stars show a P Cyg type spectrum, that is, their emission lines have blueshifted absorption features superimposed. According to Strom (1972) and Herbig (1960), the theory that this effect is caused by an expanding envelop with self absorption is widely believed.

Herbig (1960) states that the star T Tauri has a set of two absorption lines superimposed on its H and Ca emission lines, corresponding to radial velocities of -70 and -170 km/sec, and that RY Tau has one line corresponding to a radial velocity of -90 km/sec.

From an analysis of the forbidden-line radiation, coming from the small forbidden-line region surrounding T Tauri, Herbig says that Varsavsky, in 1960, finds a mass loss of about $.5 \times 10^{-5}$ $M_{\odot}$/yr for T Tauri, assuming that the forbidden-line region is 750 AU in diameter, and that the region is sustained by material rising at 170 km/sec.

The accretion of matter by some young stars is indicated

by the presence of an inverse- P Cyg spectrum (sometimes called a YY Orionis spectrum). Out of a sample of 23 UV-excess stars observed by Walker (1969) in NGC 2264, he finds 10 show an inverse P Cyg effect. None of these are T Tauri stars, but they are all closely related to T Tauri stars. In 1972, Walker (1972) reports finding two more young stars with inverse P Cyg effect, RR Tauri and θ^1C Orionis.

T Tauri spectra show a strong continuum in the visual, which is sometimes called the 'blue continuum', and a continuum starting in the $\lambda\lambda$3700-3800 region and rapidly rising toward the shorter wavelengths. Unlike the blue continuum, this UV continuum adds an appreciable amount of energy to the luminosity of the star. According to Herbig (1960), this UV continuum has been attributed to synchrotron emission like that from some solar grains, and to the running together of the higher Balmer lines. The latter of these hypotheses he refers to as Böhm's hypothesis. The higher Balmer lines blend together because of turbulent broadening, according to this hypothesis.

Mendoza (1966) finds UV excesses for the majority of the 26 stars he observes. Anderson and Kuhi (1969) give detailed observations of the T Tauri star AS 209 (1900: 16^h $43^m.6$, -14° 13'), and report that it shows a large UV excess. They say they favor Böhm's hypothesis, since Kuhi's observed line width for the Hβ line, indicates a turbulent velocity as large as 100 km/sec, which would be more than enough to blend the higher Balmer lines.

In general, Hα emission and UV excess in T Tauri stars is correlated, but for individual stars there does not appear to be a correlation between the two as the star varies in brightness. In the case of AS 209, Anderson and Kuhi looked for such a correlation, and found none.

Various correlations have been noted between observed T Tauri phenomena. Herbig finds that as RW Aur gets fainter in the V band, it gets redder. Anderson and Kuhi (1969) find that AS 209 increases its UV excess as it gets fainter in the V band. Cohen (1973a) finds that as T Tauri gets fainter in the visual it gets brighter in the near infrared.

Walker (1969) does a detailed study of SU Ori, an Inb star with inverse P Cyg spectrum and UV excess, and finds that when the redward displaced absorption feature is most prominent, the star is brightest. He shows five spectrograms of SU Ori taken when the star was at different magnitude, and the redward displaced absorption line disappears as the star gets dimmer.

Poveda (1965b, 1965c) suggests that the circumstellar shells about T Tauri stars and related objects are pre-planetary systems. He says that some of the variability of these stars must be due to eclipses by proto-planets (large clouds along the orbits of the planets-to-be), and that phenomena such as FU Orionis occur because the circumstellar material can form into large particles very rapidly (a few years); thus, rapidly dropping the optical depth of the material, and brightening the star.

In light of the observed characteristics of the T Tauri stars and related objects described above it is not surprising that there have been a number of papers published in the past few years dealing with the problem of radiative transfer in circumstellar envelopes. In each of these papers the author makes a number of assumptions about the object or objects he is attempting to model in order to simplify the radiative transfer problem. These simplifying assumptions tend to reduce the accuracy and the versatility of the resulting model and should therefore be avoided if possible.

In all of these papers it has been assumed that the envelope is spherically symmetric about the central star and that the effects of the spherical symmetry are significant. If the entire shell were metrically thin and distant from the central star it would be possible to simplify the problem by assuming the shell to be stratified into parallel planes. This simplification could also be made if the outer layers of the envelope were optically thick. However, it appears from the observations that the circumstellar clouds about the T Tauri stars and related objects can not be adequately represented by a model based on a plane parallel approximation. The assumption of spherical symmetry while much better than the simple plane parallel assumption is still an idealization since it has been pointed out that visually these objects appear to have a very complicated outer structure (e.g., Herbig, 1968).

In all these papers it is assumed that a power law of the form $K(r) = [C/r^n]$ governs either the volume absorption coefficient or the number density of particles. Here r is the distance from the central star, C is a constant, and n is a variable index (Chandrasekhar, 1934). Some assumption as to the functional relationship between K and r is necessary (see Section II), and this one seems to allow reasonable flexibility with the adjustment of only one parameter (the constant is determined by the geometry and total optical depth of the shell). In a few of these papers it is further assumed that $n = 0$; that is, that K(r) is constant with r .

Several authors (Stein, 1966; Low and Smith, 1966; Krishna Swamy, 1970) have considered the less general problem of radiative transfer in an optically thin circumstellar shell in which scattering and reabsorption of infrared radiation emitted by the dust can be neglected. Stein's paper pertains to the observed infrared excesses of certain B stars; Low and Smith's, to the much larger infrared excess of R Monocerotis and Krishna Swamy's, to the infrared excesses of several infrared objects, among them, VY Canis Majoris.

Stein in his paper states that the total optical depth of the shells he is considering is about 10^{-3}. For a shell this optically thin it is quite reasonable to assume that the star is the only significant energy source in the system. In the paper by Swamy and in the the one by Low and Smith, the objects modeled (e.g., VY CMa and R Mon) show an amount

of infrared radiation as compared with the optical which indicates that these objects have optically thick shells (Mendoza, 1966; Low et al., 1970).

Huang in one paper (Huang, 1969a) considers the two extreme cases of very small and very large optical thickness and then in a second paper (Huang, 1969b) considers the more general problem of intermediate optical thickness. In both these papers Huang makes the assumption that the opacity of the dust is proportional to the geometrical cross section of the grains.

In the first paper he solves the transfer problem for an optically thin shell in much the same manner as Stein (1966). His approach to the problem of the optically thick shell is analogous to that of Chandrasekhar (1934) for extended stellar atmospheres.

In the second paper he solves the transfer equation for a spherical shell having its inner boundary in contact with the surface of the central star, assuming grey particles, the Eddington approximation, isotropic scattering and Local Thermodynamic Equilibrium. He does not actually state that the shell is in contact with the surface of the star but that the radiation at the inner boundary of the shell is completely diffuse. For all practical purposes as long as the inner edge of the shell is within a few stellar radii of the surface of the star the radiation field can be considered diffuse.

Huang (1971) published a third paper dealing specifi-

cally with shells distant enough from their central stars such that the stars could be considered point sources. He points out in this paper that the assumption of a completely diffuse radiation field throughout the shell represents an idealized case of one extreme while the assumption that the star is a point source represents the other extreme.

In his second paper Huang (1969b) argues that the assumption that the particles scatter radiation as grey-bodies is valid. He states that in the case of interstellar reddening blue light is preferentially scattered out of the line of sight, whereas in the case of a circumstellar dust cloud we observe scattered radiation coming in all directions; such that, the amount of radiation of a certain wavelength which is lost in direct transmission along the line of sight is regained due to the overall scattering process.

For his intermediate case Huang (1969b) assumes that the radiation field can be broken into two parts - a visual part and an infrared part. He then proceeds to solve the overall transfer problem as though it were two less difficult problems: (1) a nonconservative scattering problem involving only the stellar radiation in the visual (the infrared emission of the star is assumed to be negligible) and (2) the problem of an atmosphere in local thermodynamical equilibrium for the infrared radiation emitted by the dust, with an energy source, namely, the visual radiation absorbed in the nonconservative optical region. Therefore, the results for his intermediate case described in his

second and third papers (Huang, 1969b, 1971) refer to these two broad wavelength regions.

In his results Huang (1971) states that the radiation field and the temperature distribution do not critically depend upon the index n in the expression assumed for the density distribution and indirectly that the ratio of the inner to the outer radii of the shell is an unimportant factor. In Section IV it is shown that these results are not in general correct.

Huang does not apply this method to any observed object, but in 1970 Herbig (1970) uses it successfully in the development of a model for VY Canis Majoris, and recently Apruzese (1974) has used it to model the infrared object HD 45677 (a Be star with a large infrared excess). The approach followed by Apruzese parallels Huang's for the intermediate case and diffuse radiation except that he modifies Huang's technique slightly to allow the determination of the radiation field in ten spectral regions to the blue side of 1μ . For each of these spectral regions he has in effect a problem of nonconservative scattering. Apruzese's model will be considered further in Section IV.

Larson (1969b) in studying the emission of collapsing protostars finds an approximate solution for the radiative transfer in a spherical dust shell in which the particles scatter none of the radiation but absorb an amount proportional to λ^{-p}, where λ is the wavelength and p is a variable index. He derives an approximate expression for the

temperature distribution in the cloud and using this solves for the emitted spectrum. The weighting function integration method he develops to compute the emitted spectrum from the known temperature distribution is also used by Herbig in the paper mentioned above. For the index n which is used to establish the density distribution in the cloud Larson uses 1.5 and states that this is the value determined by his dynamical calculations and published in a previous paper (Larson, 1969a).

Hummer and Rybicki (1971) have a procedure involving iteration on the Eddington factor, K/J, which they use to solve the transfer problem, under the assumption of the conservative grey case, for a spherical cloud extending from a point of radiation at its center out to some finite radius, R.

None of the papers mentioned above adequately deal with the problem of radiative transfer in circumstellar envelopes of intermediate optical depth. The only two procedures that come close to solving this case are those due to Huang (1969b, 1971), Larson (1969b), and Apruzese (1974). They all assume that the density in the shell is proportional to $1/r^n$ and Huang and Apruzese assume that the particles are isotropic scatters - Larson neglects scattering. The first of these assumptions seems as good as any other for the density distribution and is not critical to the solution of the problem. The second assumption is necessary in order to take advantage of the spherical symmetry of the

shell. It allows us to reduce the problem to one involving only two spacial coordinates. If the particles are assumed to scatter according to an arbitrary phase function the problem becomes much more complex. Huang assumes that the opacity of the cloud is due to the geometrical cross section of the particles and therefore that it is grey, whereas, Apruzese and Larson assume that the opacity is wavelength dependent. The procedure described by Huang is restricted to cases where the central star can be considered a point source or the radiation is completely diffuse. It is further restricted to cases where the Eddington approximation is valid. Most importantly his procedure does not describe the radiation field at a particular wavelength but merely breaks it into two regions - visual and infrared. The procedure described by Apruzese is based on Huang's procedure and involves one major improvement - his procedure can be used to determine the radiation field at a number of wavelengths in the visual. Larson's procedure, as well as neglecting scattering, uses a rather crude approximation for the temperature distribution in the shell. His procedure does however allow the determination of the spectral-energy distribution emergent from the shell in the visual and infrared.

In Sections II and III a technique is developed capable of solving the transfer problem for the radiation field at any point in a circumstellar shell, for any wavelength, and any optical depth.

This technique is applicable to cases where the central star can be considered neither a point source nor a diffuse source of radiation. To simplify the problem the following assumptions are made: (1) the cloud is spherically symmetric about the central star, (2) the cloud is made of small particles which have no preferential orientation, (3) the particles reemit absorbed radiation isotropically and scatter radiation isotropically, (4) the particles have an albedo which is independent of wavelength, (5) the particles radiate as grey-bodies at a temperature T where T is a function of the radiation field about the particle, (6) the volume absorption coefficient as a function of the distance from the central star, K(r), is constant with wavelength and proportional to the density $\rho(r)$, and (7) the optical depth τ and the distance from the central star are related by the usual expression (Chandrasekhar, 1934),

$$d\tau = - b \frac{dt}{t^n} \; ; \; t = \frac{r}{R} \; ,$$

where b is a constant.

This technique characterizes each dust shell by a set of parameters related to the size of the shell and the density distribution within the shell, the size and temperature of the central star, and the albedo of the dust particles within the shell. The equation of transfer is solved in integral form by a computer code using an iterative procedure.

SECTION II
BASIC RELATIONS

In this section the physical and mathematical relations necessary to solve the transfer equation for the radiation field in a circumstellar dust cloud will be developed. These relations will be in terms of a number of physical parameters that characterize the dust cloud.

The parameters to be used can be placed into three groups, one that specifies the geometry of the cloud, one that specifies the albedo of the particles, and one that specifies the temperature of the central star. The first group consists of five parameters, the radius of the central star, the inner radius of the cloud, the outer radius of the cloud, the total optical depth of the cloud, and an index which specifies the density distribution. These five quantities will be designated respectively as R_*, R_I, R, τ_I, and n. The second and third groups have only one member each: the albedo of the particles, designated ω_o, in the case of the second group and the temperature of the central star, designated T_*, in the case of the third.

For some set of these seven parameters the dust cloud model should be capable of reproducing the observed spectral-energy distribution of an object such that that set of parameters can be considered to characterize the observed object.

Consistent with the simplifying assumptions set forth in Section I, relations can be derived for a number of useful quantities. Using the expression for $d\tau$ given in Section I we can derive the relation for the absorption per unit volume at a distance r from the central star, K(r). We have

$$dr = Rdt$$

$$d\tau = - \frac{bR^{n-1}dr}{r^n} \quad ,$$

but

$$d\tau = K(r)dr,$$

and therefore,

$$K(r) = - \frac{bR^{n-1}}{r^n}$$

or

$$K(r) = \frac{B}{r^n} \quad , \qquad (1)$$

where B is a constant. We can also derive expressions for the optical depth at r, $\tau(r)$, and for B in terms of R_I, R, τ_I, and n. In the following $n \neq 1$ unless specified otherwise. We have

$$\tau(r) = \int_o^r K(r)dr$$

or

$$\tau(r) = B\int_o^r r^{-n}dr \quad ,$$

and, therefore,

$$\tau(r) = B\left(\frac{r^{1-n}}{1-n} \right) + C \quad , \qquad (2)$$

where C is a constant of integration. Since $\tau(R_I) = \tau_I$ and

$\tau(R) = 0$ we have

$$\tau_I = B \left(\frac{R_I^{1-n}}{1-n} \right) + C \qquad (3)$$

and

$$0 = B \left(\frac{R^{1-n}}{1-n} \right) + C \qquad (4)$$

from which we obtain,

$$C = - B \left(\frac{R^{1-n}}{1-n} \right).$$

Substituting this into (3) we have for τ_I,

$$\tau_I = B\left(\frac{R_I^{1-n}}{1-n} \right) - B\left(\frac{R^{1-n}}{1-n} \right)$$

or

$$\tau_I = \frac{B}{1-n} (R_I^{1-n} - R^{1-n}).$$

So

$$B = \frac{\tau_I(1-n)}{(R_I^{1-n} - R^{1-n})}$$

and we obtain from equation (1)

$$K(r) = \frac{\tau_I(1-n)}{(R^{1-n} - R_I^{1-n})r^n}, \text{ if } R_I \leq r \leq R \qquad (5)$$

$$= 0, \text{ if } r > R, \text{ or } r < R_I$$

and from equation (2)

$$\tau(r) = \frac{\tau_I(R^{1-n} - r^{1-n})}{(R^{1-n} - R_I^{1-n})}. \qquad (6)$$

In the case with constant density we have n = 1 and the relations for K(r) and $\tau(r)$ become

$$K(r) = \tau_I[\ell n(R/R_I)r]^{-1}, \quad R_I \leq r \leq R$$

$$= 0, \quad r > R, \quad r > R_I \tag{7a}$$

$$\tau(r) = \tau_I \ell n(R/r) \; [\; n(R/R_I)\;]^{-1} \tag{7b}$$

Equations (6) and (7b) apply only for $R_I \leq r \leq R$. For $r < R_I$, $\tau(r) = \tau_I$, and for $r > R$, $\tau(r) = 0$.

The spectral-energy distribution is observed in terms of flux received at the surface of the earth per unit wavelength, so this is the quantity we want to calculate with our model. If we define $F(\lambda,r)$ as the flux at wavelenth λ through a unit area of the shell of radius r about the central star, where $F(\lambda,r)$ is in units of ergs/cm^2 - λ - str - sec, we have

$$F(\lambda,D) = F(\lambda,R)R^2/D^2 \; ,$$

where D is the distance between the object and the earth. Note that if D is not a known quantity we can still find a scaled flux and thus determine at least the shape of the spectral-energy distribution.

We also have

$$F(\lambda,r) = \int_{\omega} I(\lambda,r,\omega)\cos\theta \; d\omega \; , \tag{8}$$

where $I(\lambda, r, \omega)$ is the specific intensity of radiation at wavelength λ, at any point a distance r from the central

star, and coming from some direction ω radians from the central star. The integration is over 4π steradians. Because of our assumption of spherical symmetry we can define I uniquely with reference to only two of the three spherical coordinates, r and θ; there will be no ϕ dependence. It is also true that $I(\lambda, r, \theta) = I(\lambda, r, -\theta)$, so the integration over θ need only be carried out from 0 to π. Thus,

$$F(\lambda,r) = 2\pi \int_0^{\pi} I(\lambda,r,\theta)\sin\theta \cos\theta \quad d\theta$$

where θ is an angle in a single plane.

In order to determine $F(\lambda,r)$ and the $F(\lambda,D)$ we must be able to calculate $I(\lambda,r,\theta)$ numerically. This can be expressed as

$$I(\lambda,r,\theta) = \int_0^{\tau_m} e^{-t}\, S(\lambda,r_e,\theta_e)\,dt, \qquad (9)$$

where $S(\lambda,r_e,\theta_e)$ is the source function for radiation of wavelength λ, emitted in a direction θ_e radians from the central star, at any point a distance r_e from the central star. The integration is carried out over optical depth along the line of sight, from a point at a distance r from the central star and in a direction θ radians from the central star. The upper limit for the integration, τ_m, represents the maximum optical depth attainable along the line of sight and will always be less than $2\tau_I$. The quantities r_e and θ_e are functions of r, θ and t. Here t is optical depth along the line of sight and the variable of integration. Thus we have $r_e = r_e(\theta,r,t)$ and $\theta_e = \theta_e(\theta,r,t)$.

The expression for $I(\lambda,r,\theta)$, given in equation (9),

does not help us unless we can evaluate $S(\lambda,r_e,\theta_e)$. The source function can be expressed as the ratio of the emission to the absorption coefficient, that is,

$$S(\lambda,r_e,\theta_e) = j(\lambda,r_e,\theta_e)/K(r_e),$$

where $j(\lambda,r_e,\theta_e)$ gives the emission per unit volume at a distance r_e from the central star, at wavelength λ, and in a direction θ_e radians from the central star. Since the dust model is based on the idea that the dust scatters part of the radiation it intercepts and absorbs and reradiates the rest, we can write $S(\lambda,r_e,\theta_e)$ in the following form:

$$S(\lambda,r_e,\theta_e) = [j_B(\lambda,r_e,\theta_e) + j_s(\lambda,r_e,\theta_e)] \; / \; K(r_e) \; , \qquad (10)$$

where $k(\lambda,r_e,\theta_e)$ has been broken into two parts, scattered emission and thermal or grey-body emission, designated respectively j_s and j_B .

It is evident that both emission terms in equation (10) are related to the radiation field, $I(\lambda,r_e,\theta)$, at r_e. Therefore, we need to determine the exact functional relationships expressing $j_B(\lambda,r_e,\theta_e)$ and $j_s(\lambda,r_e,\theta_e)$ in terms of $I(\lambda,r_e,\theta)$. In doing this we will first need to derive expressions for $r_e = r_e(\theta,r,t)$ and $\theta_e = \theta_e(\theta,r,t)$.

From consideration of the geometry in Figure 1, we have

$$r_e(\theta,r,t) = (r^2 + s^2 - 2rs\cos\theta)^{1/2}, \qquad (11)$$

where s is the metric distance along the line of sight to the point of emission and

$$\theta_e = \sin^{-1} [(r/r_e)\sin\theta].$$

The variable of integration along the line of sight, t, can be evaluated from the expression

$$t = \int_o^s K(r)\, ds \qquad (12)$$

once we have assigned a value to n in the formula for K(r).

The amount of radiation scattered by a particle will be that amount which is intercepted by the cross sectional area of the particle and not absorbed; that is, the amount intercepted times ω_o. The amount of this radiation scattered in a direction θ_e will, in general, be given by

$$j_s(\lambda, r_e, \theta_e) = (k_p \omega_o / 4\pi) \int_\omega P(\alpha) I(\lambda, r_e, \theta)\, d\omega, \qquad (13a)$$

where k_p is the cross sectional area of the particle and $P(\alpha)$ is a phase function defined such that

$$(1/4\pi) \int_\omega P(\alpha)\, d\omega = 1 .$$

The quantity α is the angle through which the radiation is scattered and is thus a function of θ at r_e and of θ_e (see Figure 1).

Since we are assuming isotropic scattering, where $P(\alpha) = 1$ for all α, we can drop θ_e from our notation and rewrite equation (13a) as

$$j_s(\lambda, r_e) = (k_p \omega_o / 4\pi) \int_\omega I(\lambda, r_e, \theta)\, d\omega . \qquad (13b)$$

Equation (13b) gives the radiation scattered per particle and we want the radiation scattered per cm^3. To derive the

needed form we must replace k_p in equation (13b) with the cross sectional area of all the particles in a cm^3, which we will denote k. Then,

$$j_s(\lambda,r_e) = (k\omega_o/4\pi) \int_{\omega} I(\lambda,r_e,\theta)\,d\omega$$

which because of spherical symmetry we can rewrite as

$$j_s(\lambda,r_e) = (k\omega_o/2) \int_{o}^{\pi} I(\lambda,r_e,\theta)\sin\theta\ d\theta. \quad (14)$$

Two additional equations for j_s are formed by separating $I(\lambda,r_e,\theta)$ into a term due to the cloud and a term due to the star. Let $\gamma(\theta)$ be defined such that $\gamma(\theta) = 1$ if $0 \leq \theta \leq \theta_*(r_e)$ and $\gamma(\theta) = 0$ if $\theta > \theta_*(r_e)$, where $\theta_*(r_e) = \sin^{-1}(\frac{R_*}{r_e})$ is the angular radius of the central star as seen from a distance r_e; then

$$I(\lambda,r_e\theta) = I_c(\lambda,r_e,\theta) + \gamma(\theta)\ I_*(\lambda)\ .$$

In the above equation I_c, the term due to the cloud, is given by

$$I_c(\lambda,r_e,\theta) = \int_{o}^{\tau_c} e^{-t}\ S(\lambda,r)\ dt$$

where $r = r(\theta,r_e,t)$ is obtained analogously to r_e (see equation 11),

$$\tau_c = \tau_m - \gamma(\theta)\quad(\tau_b - \tau_m)$$

and τ_b represents the optical depth along the line of sight to the inner boundary of the cloud. The term due to the star is $I_*(\lambda) = e^{-\tau_b}B(\lambda,T_*)$, where $B(\lambda, T_*)$ gives the Planckian emission of the star.

From equation (14) and the above expression for I we have

$$j_s(\lambda,r_e) = (k\omega_o/2)\left[\int_o^{\pi} I_c(\lambda,r_e,\theta)\sin\theta\, d\theta + \int_o^{\theta_*} I_*(\lambda)\sin\theta\, d\theta\right], \quad (15a)$$

and if we are only interested in the bolometric emission, we have

$$j_s(r_e) = (k\omega_o/2)\left[\int_o^{\pi} I_c(r_e,\theta)\sin\theta\, d\theta + \int_o^{\theta_*} e^{\tau_e-\tau_I}\left(\frac{\sigma T_*^4}{\pi}\right)\sin\theta\, d\theta\right], \quad (15b)$$

where

$$I_c(r_e,\theta) = \int_o^{\infty} I(\lambda,r_e,\theta)d\lambda, \text{and } \sigma \quad (15c)$$

is the Stefan-Boltzmann constant.

When θ_* is very small we can use the following approximate versions of equations (15a) and (15b):

$$j_s(\lambda,r_e) = (k\omega_o/2)\int_o^{\pi} I_c(\lambda,r_e,\theta)\sin\theta\, d\theta + (k\omega_o/4\pi)\exp(\tau_e-\tau_I)R_*^2\pi B(\lambda,T_*)/r_e^2 \quad (16a)$$

and

$$j_s(r_e) = (k\omega_o/2)\int_o^{\pi} I_c(r_e,\theta)\sin\theta\, d\theta + (k\omega_o/4\pi)\exp(\tau_e-\tau_I)R_*^2\,\sigma T_*^4/r_e^2 \quad (16b)$$

where τ_e is the optical depth from the surface of the cloud to r_e and the other quantities used have been previously defined.

We now turn to the problem of determining the grey-body emission of the particles, $j_B(\lambda, r_e, \theta)$. As long as any elemental volume is small enough for every particle in it to experience nearly the same radiation field, the amount of energy absorbed will be independent of the shape of the element and its orientation. This absorbed energy will be a function of I and the effective cross sectional area of the particles per unit volume, k. Thus, we can derive an expression for k by considering the energy absorbed by an idealized unit volume; namely a small cylinder of unit height and unit cross sectional area oriented such that the incident radiation is perpendicular to one end.

For such a cylinder the amount of the intensity lost due to absorption, I_L, will be $I_L = I(1 - e^{-\tau})$, where τ here is the total optical depth along the axis of the cylinder, or if we assume the medium to be thin enough so that occultation of one particle by another are rare, we have $I_L = (A_{part}/A_{cy})I$, where A_{part} and A_{cy} respectively denote the cross sectional areas of the particles and the cylinder. Now we can write

$$A_{part} = (1 - e^{-\tau})A_{cy} ,$$

and since $\tau << 1$, we have

$$A_{part} = [1 - (1 - \tau)]A_{cy} = A_{cy}\tau ,$$

or

$$A_{part} = A_{cy}K(r)\ h ,$$

where h is a length over which we have an optical depth τ and

K(r) has been assumed constant over this length. For a cylinder of unit volume we can take $A_{cy} = 1$ and $h = 1$; then A_{part}/unit vol = K(r), and k(r) = K(r).

We now need to derive a relation between the effective cross sectional area of the particles in a volume and the effective surface area enclosing that volume. Let A be the sum of the effective surface areas of all the individual particles in a volume element V and let k be the sum of their effective cross sectional areas. Define the effective cross sectional area of a single particle, to be its geometrical cross sectional area averaged over all possible orientations. Now if the number of particles in V is large, and they have no preferential orientation; then k will not vary with the direction of observation ω, and we will be able to derive a relation for A in terms of k; thus defining A.

For the volume, V, the energy absorbed, E_a, is given by the relation

$$E_a = \int_{\omega} I(\omega) k \, d\omega \ ,$$

if the density is low enough such that occultations of one particle by another can be neglected. The energy emitted, E_e, is given by $E_e = \sigma T^4 A$. Therefore,

$$\int_{\omega} I(\omega) k \, d\omega = \sigma T^4 A \ ,$$

if the particles are in thermal equilibrium with the radiation field. This can be rewritten as

$$T^4 = (k/A\sigma) \int_{\omega} I(\omega)\, d\omega \ , \qquad (17)$$

and if we let W = k/A, we have

$$T^4 = (W/\sigma) \int_{\omega} I(\omega)\, d\omega \ . \qquad (18)$$

This equation is true for any volume of particles and any radiation field.

If we apply equation (18) to a volume situated in a black-body cavity at temperature T_B, we have

$$T_B^4 = (W/\sigma) \int_{\omega} B(T_B)\, d\omega,$$

and since $B(T_B)$ is constant with ω, we have

$$T_B^4 = [W4\pi B(T_B)]/\sigma \ . \qquad (19)$$

Since $B(T_B)$ is not a function of λ, it represents the Planckian integrated over λ. Thus,

$$B(T_B) = \int_0^{\infty} B(\lambda, T_B)\, d\lambda = (\sigma T_B^4)/\pi \ ,$$

and equation (19) becomes $T_B^4 = 4WT_B^4$, from which we obtain W= 1/4, a value indentical to that obtained for a sphere.

Substituting this value for W into equation (18) gives us

$$T = [(1/4\sigma) \int_{\omega} I(\omega)\, d\omega]^{1/4}.$$

This equation can be used to find the temperature of any grey-body due to an arbitrary radiation field, $I(\omega)$, provided that the body is tumbling randomly.

Since W is the ratio of the effective cross sectional

area to the effective surface area of a particle, $A = 4k_p$ for any particle.

From our assumptions that the particles have no preferential orientation and that they are in thermal equilibrium with the radiation field, we have that $A = 4k_p$, and that

$$F(\lambda,T) = (1 - \omega_o)\pi B(\lambda,T) \ ,$$

where A is the effective surface area of a particle, T is the equilibrium temperature of the particle, $B(\lambda,T)$ is the Planckian and $F(\lambda,T)$ is the flux per unit effective area of the particle. The thermal isotropic emission of a single particle can now be written as

$$j_B(\lambda) = (A/4\pi)F(\lambda,T) \ ,$$

or

$$j_B(\lambda) = k_p(1-\omega_o)B(\lambda,T) \ .$$

The corresponding emission for a unit volume of such particles will be

$$j_B(\lambda,r_e) = K(r_e)(1-\omega_o)B(\lambda,T) \ .$$

Note that the temperature T, like K, is a function of the distance from the central star, r.

If this emission is considered only bolometrically,

$$F(T) = (1-\omega_o)\sigma T^4 \ ,$$

and

$$j_B(r_e) = [K(r_e)/\pi](1-\omega_o)\sigma T^4 \quad . \qquad (20)$$

The condition of thermal equilibrium gives us the relation

$$E_a(r) = E_e(r) \quad , \qquad (21)$$

where $E_a(r)$ and $E_e(r)$ denote, respectively, the energy absorbed and emitted by a unit volume of particles at a distance r from the central star. Now from equations (20) and (21) we have

$$E_a(r) = \int_\omega (1-\omega_o)(\sigma/\pi)K(r)T^4(r)\,d\omega \quad ,$$

and since the emission is isotropic

$$E_a(r) = 4K(r)\ (1-\omega_o)\sigma T^4(r) \quad .$$

From this formula for E_a we can obtain the following expression for the temperature,

$$T(r) = \{[1/4\sigma(1-\omega_o)][E_a(r)/K(r)]\}^{1/4} \quad ,$$

For the non-bolometric case we have,

$$E_a(r) = K(r)\ (1-\omega_o) \iint_{\omega\lambda} I(\lambda,r,\theta)\,d\lambda d\omega \quad ,$$

giving us

$$T(r) = [(1/4\sigma) \iint_{\omega\lambda} I(\lambda,r,\theta)\,d\lambda d\omega]^{1/4} \quad .$$

Because of spherical symmetry we can write this as

$$T(r) = [(\pi/2\sigma) \int_o^\pi \int_\lambda I(\lambda,r,\theta)\sin\theta\ d\lambda\ d\theta]^{1/4} \quad .$$

If we divide the radiation field into two parts, as

we did before, we have

$$T(r) = \{(1/4\sigma)[2\pi \int_0^{\pi} I_c(r,\theta)\sin\theta\, d\theta + \int_0^{\theta_*} \frac{\sigma T_*^4}{\pi} e^{\tau-\tau_I} \sin\theta\, d\theta]\}^{1/4}, \qquad (22)$$

where $I_c(r,\theta)$ is the bolometric intensity defined by equation (15c). When the central star can be considered a point source we have the additional equation,

$$T(r) = \{(1/4\sigma)[2\pi \int_0^{\pi} I_c(r,\theta)\sin\theta\, d\theta + e^{(\tau-\tau_I)} (R_*^2\sigma T_*^4/r^2)]\}^{1/4}.$$

Note that in equation (9) I is a functional of S and that in equation (10a) S is a function of j. We have seen that j is a functional of I; therefore, I is a functional of S and S is a functional of I. Thus, equations (9) and (10a) can be rewritten as a recurrence formula for $I(\lambda,r_e,\omega)$, which can be used in an iterative solution for the radiation field throughout the cloud and hence for the desired spectral-energy distribution.

The recurrence formula is

$$I_n(\lambda,r,\omega) = \int_0^{\tau_m} e^{-t} S[\int_{\omega} I_{n-1}(\lambda,r_e,\omega)\, d\omega]dt, \qquad (23)$$

where the subscripts n and n+1 refer to iterations n and n+1. The true radiation field consistent with a given set of parameters will be given by

$$I(\lambda,r,\omega) = \lim_{n\to\infty} I_n(\lambda,r,\omega) \quad .$$

This completes the definition and derivation of the basic quantities needed to implement an iterative solution of equation (11).

Once the proper set of the parameters, τ_I, R_I, R and n, is determined, we can obtain values for the density within the cloud, $\rho(r)$, and the total mass of the cloud M.

If we let D equal the number of particles per cm^3 and d equal the average diameter of a particle, where $d << R$, then

$$D = \frac{CSA/cm^3}{CSA/particle} = particles/cm^3 \ .$$

The cross sectional area of the particles per cubic centimeter is a function of r and is given by K(r); thus,

$$D(r) = \frac{K(r)}{\pi(\frac{d}{2})^2} = \frac{4}{\pi} K(r) d^{-2} \ .$$

For the volume and mass of a particle, V_p and m_p respectively, we have

$$V_p = \frac{4}{3} \pi (\frac{d}{2})^3 \ cm^3/particle,$$

and

$$m_p = \rho_p \frac{4\pi}{3} (\frac{d}{2})^3 \ grams/particle \ ,$$

where ρ_p is the specific gravity of a grain. The density of the cloud at a distance r from the central star will then be given by

$$\rho(r) = D(r) \ m_p$$

$$\rho(r) = \frac{4}{3}\pi\left(\frac{d}{2}\right)^3 \rho_p \frac{K(r)}{\pi\left(\frac{d}{2}\right)^2} \text{ , or}$$

$$\rho(r) = \frac{4}{3}\rho_p K(r)\left(\frac{d}{2}\right) .$$

Substituting for K(r), we find

$$\rho(r) = \frac{2}{3}\rho_p d \left[\frac{\tau_I(1-n)}{R^{1-n}-R_I^{1-n}}\right] \frac{1}{r^n} . \qquad (24)$$

From the above expression for $\rho(r)$ we can derive an expression for the total mass of the cloud. We have

$$M = \int_{R_I}^{R} (4\pi r^2)\rho(r)dr ,$$

from which we obtain,

$$M = \frac{8\pi\rho_p\tau_I(1-n)(R^{3-n} - R_I^{3-n})d}{3(3-n)(R^{1-n} - R_I^{1-n})} . \qquad (25)$$

SECTION III
NUMERICAL PROCEDURE

In this section a procedure based on the equations of Section II is developed, to effect a numericsl solution for the radiation field in the dust shell. This procedure will involve iterative numerical integrations of equation (23) to obtain a set of convergent series of $I_n(\lambda, r_i, \omega)$. Here i specifies the i^{th} such set and r_i, therefore specifies the distance from the central star at which the $I(\lambda, r_i, \omega)_n$ for that set are to be evaluated. The n signifies that this is a value obtained in the n^{th} iteration. All the integrations will be performed using Gauss-Legendre formulas.

In order to accomplish the necessary integrations it will first be necessary to establish an integration grid in keeping with the boundary conditions imposed by the geometry of the shell and the central star. Consider the spherical shell of dust extending from R_I to R and divided into N thinner concentric shells each with the same optical thickness, τ_I/N (see Figure 2). The inner and outer radii of these shells are a function of τ and can thus be found from the equation

$$r(\tau) = [R^{1-n} - (\tau/\tau_I)(R^{1-n} - r_I^{1-n})]^{\frac{1}{1-n}} \qquad (26)$$

For each of the N points lying on the semi-diameter of the cloud, $\overline{SR}$, (see Figure 2) at distance r_i from the central star, we assign M values of the angle θ, which will define M lines radiating from each point. We then break these radial lines into segments of approximately equal optical depth, where the end points of the segments are all the points at which the radial lines intersect the N circles of radii r_i.

Thus, about each of the N points on $\overline{SR}$ we have M radial lines, and each of these lines is broken into from 1 to 2N segments, where the actual number of segments for any particular line depends on how many of the N circles of radii r_i that line intersects.

The M values of θ used at each of the N points along $\overline{SR}$ would in general be the Gauss-Legendre points for the interval 0 to π; however, it is usually advantageous to break this interval into two intervals with M/2 Gaussian points each - one from 0 to $\theta_m(r_i)$ and the other from θ_m to π, where $\theta_m(r_i)$ is an angle that must be determined for each of the N points r_i. If r_i is small enough so that the central star shows an appreciable disk, then $\theta_m(r_i)=\theta_*(r_i)$, but if r_i is large enough so that the star can be considered a point source $\theta_m(r_i)$ will be an angle between 0 and $\pi/2$. The value of $\theta_m(r_i)$ in this case should be determined, such that, it lies between $\pi/2$ and the value of θ at which $I(r_i,\theta)$ has its greatest value. Defining $\theta_m(r_i)$ in this manner allows us to concentrate our Gaussian points on the part of the interval

0 to π where $I(\theta)$ is varying most rapidly. In one special case the M Gaussian points must be determined in a different manner. When $r_i = r_n = R$ the M θ's are restricted to the interval 0 to $\pi/2$ since for $\pi/2 < \theta < \pi$, $I(R,\theta)$ obviously vanishes.

We have broken each of the M radial lines into segments as a first step in the determination of the locations of L Gaussian points to be used in the numerical evaluation of equation (23). Figure (2) shows a few representative radial lines for the i^{th} of the N points on $\overline{SR}$. Also, the radial lines are shown broken into segments with end points a distance s_k from $\overline{SR}$, where s_k is measured along the radial line and k is an index ranging from 1 to 2N.

Let x and y be the rectangular coordinates of a point in a right-handed coordinate system, where the central star is the origin, and the semi-diameter $\overline{SR}$ is the positve y-axis. Also, let the slope and y-intercept of a radial line be denoted by m and b respectively; then, each pair of values for m and b defines a particular radial line. In terms of previously defined quantities, $m = \text{Cot}\ (\theta)$ and $b = \bar{r}_i$. When b and m are specified, the rectangular coordinates of all the points where a particular radial line intersects the N circles of radii r_i can be found by solving, for x and y, the system of equations

$$x^2 + y^2 - r_i^2 = 0$$

$$y - mx - b = 0, \text{ for } i = 1 \text{ to } N.$$

We are only interested in points to one side of $\overline{SR}$, so we exclude all solutions with $x > 0$. Points which are occulted by the star are also excluded.

The starting point of a radial line will lie on $\overline{SR}$, and have coordinates $x = 0$ and $y = r_i$; the k^{th} point of intersection on that line will have coordinates x_k and y_k. Thus, the distance along the line from the starting point to the k^{th} point, which is denoted s_k in Figure 2 , is

$$s_k = [x_k^2 + (r_i - y_k)^2]^{-1/2} .$$

To accomplish the integration of equation (23) we must first perform the integration indicated by equation (12) along each of the radial lines using the end points of the segments on these lines as the limits of integration. Equation (11) is used here to find the distance from the central star to a point on the line and hence the values of K(r) needed by (12) from (5) or (7a).

From (12) we will obtain for each of the N x M lines of sight (LOS) a set of accurate optical depths, t_k, and corresponding distances, s_k, measured along the LOS. Because of the discontinuity caused by the central region of the dust cloud ($r < RNR$) it is helpful to break the LOS into two intervals to consist of L/2 Gaussian points.

Unless the LOS intersects the central region of the cloud ($r = r_1 = RNR$), the midpoint of each LOS, at which we can break the LOS into two segments, is roughly determined by dividing the total number of points by two. However, if

the shell r_1 is crossed two "midpoints" are established (say, MID1 and MID2) where the first such point is the point of intersection of the LOS and r_1 closest to the starting point and the second is the next point further along the LOS. The segments from the beginning of the LOS to MID1 and from MID2 to the intersection of the LOS with r_1 are to be considered the two halves of the LOS (see Figure 2). One additional case remains; if the LOS crosses the shell r_1 and then intersects the surface of the star ($r = R_*$) the LOS is to be considered terminated at r_1. This will obviously occur whenever $\theta(r_i) < \theta_*(r_i)$ for a LOS.

Next each half of the LOS is broken into 19 segments (this is the specific number used in the present version of the computer code - it can be varied if necessary) as nearly the same length in optical depth as computing time will allow (the computer code is given a parameter which sets the precision desired). This is done by an iterative procedure in which the computer code uses an Aitken-Lagrange interpolation routine (Hildebrand, 1956; Mullen, 1974) to interpolate in the table of s_k and t_k values for the set of s_k values corresponding to a new set of evenly spaced t_k values. A Gaussian integration routine is then used to evaluate equation (12), thus redetermining the values of t_k. If the values of t_k found by this integration are not equally spaced (to the precision requested) another interpolation and integration are performed, and this process is continued until the desired accuracy in spacing is achieved.

If the original set of s_k and t_k values contains only two points (the case where the LOS starts at the outer boundary r_n and then intersects r_n without intersecting r_{n-1}) the procedure described above breaks down since a set of two points can have no midpoint. In this special case the code sets up a more extensive table containing 20 points (midpoint at 10) by breaking the interval s_2 to s_1 into 19 equal segments thus obtaining 20 s_k values and then finds the corresponding t_k values by integration. The resulting tables of 20 s_k values (equally spaced) and t_k values (unequally spaced unless n = 0 in density relation) are then used in the iterative process to find the set of t_k values at equal spacing in optical depth.

Since we want to evaluate equation (23) by Guassian quadrature we must be able to evaluate the integral at the Gaussian points, t_{kg}, on the interval 0 to τ_m; therefore, we next interpolate in our table of s_k and t_k values for the s_k values, designated s_{kg} corresponding to the t_{kg} values.

We have that $S(t) = S(\tau(t))$, where τ is the optical depth measured from the outer boundary of the cloud to the point specified by t; therefore, we want to find those values of τ which correspond to the t_{kg}. From the s_{kg} determined by interpolation we can calculate, using the law of cosines, a set of corresponding r_{kg} values and from them a set of τ_{kg} values. We can then find the values of $S(\tau_{kg})$ by interpolating in a table of $S(\tau_i)$, where τ_i is the optical

depth at the i^{th} of the N shells. All the interpolations mentioned above are performed by the same Aitkin-Lagrange interpolation routine.

The table of N values of $S(\tau_i)$ is of course based on the previous iteration of the code.

The computation to determine sets of $T(r_i)$, $K(r_i)$, $S(r_i,\theta,\lambda)$, $I(r_i,\theta,\lambda)$ and ultimately $F(r_N,\lambda)$ starts from a set of initial values of $T(r_i)$, which should be as close to the expected final values as possible, and a set of the presumed physical parameters. The set of $K(r_i)$ can be found immediately from the given parameters using either equation (5) or (7a). Using the $K(r_i)$, the initial set of $T(r_i)$ and their associated optical depths, we can evaluate the integral in equation (23) along each of the M lines radiating from each of our N points. Then from the M values of $I(r_i,\theta,\lambda)$ obtained about each of the N points, improved sets of T and S can be calculated.

This process is repeated until successive sets of $T(r_i)$ converge to within a few tenths of a degree. The sets of T, K, S, and I obtained in the last iteration are taken as the true values for the cloud. A set of $F(r_N,\lambda)$ is obtained from the $I(r_N,\theta,\lambda)$ using equation (8).

To save computation time a bolometric case with ω_o = 0.0 is run to determine the set of $T(r_i)$. If in the numerical procedure, we are performing the calculations for L values of λ, then the computation time will be cut by a factor of approximately 1/L when we drop the λ dependence

and run a bolometric computation. When we use the bolometric expressions instead of their wavelength dependent analogs, equation (23) becomes the bolometric expression

$$I(r,\theta)_{n+1} = \int_{o}^{\infty} e^{-t}\, S[I(r,\theta)_{n}]\, dt.$$

Like equation (23) this can be solved iteratively for the specific intensity. The set of $T(r_i)$ is then found from equation (22) and used as the set of initial values in the desired wavelenth dependent solution.

Note that we can assume that the temperatures determined by a bolometric computation are the same as those that would result from a detailed many wavelength computation only if the particles in the cloud are grey-bodies. If we want to consider cases where $\omega_o = \omega_o(\lambda)$ then we can not use a bolometric computation to determine the temperature distribution.

The basic equations in Section II which involve integration over θ can be rewritten such that the integrations are over $\mu = \cos\theta$ by making the change of variable $\theta = \cos^{-1}(\mu)$; $d\theta = - d\mu/\sin\theta$. The code has been tested with these equations programed with θ as the variable of integration and with $\cos\theta$ as the variable of integration - the results do not differ significantly.

When the central star can not be considered a point source it is necessary to integrate over the angular diameter of the star. Since the specific intensity of the stars' surface can be considered constant (we can ignore the small

effects of limb darkening) an integration from $\theta = 0$ to $\theta = \theta_*(r_i)$ need only be done once for each r_i and used in place of the relevant point - source approximation.

For a shell very close to the star the correct contribution by the star to the mean intensity and the approximate value can differ by as much as a factor of 2.0 - the point - source approximation giving the lower value. The mean intensity, J, the Eddington flux, H, and the so-called K-integral, K, are all moments of the mean intensity I (Mihalas, 1970) that is, $M(n) = \frac{1}{2} \int_{-1}^{1} I(\mu)\mu^n d\mu$, where $I = M(0)$, $H = M(1)$, and $K = M(2)$. The flux F should not be confused with H; they are related such that $F = 4\pi H$. When RNR >> R_* we need not worry about inaccuracies due to approximating the star as a point source. For example, when $R_* \sim 0.2 \times 10^{13}$ and RNR $\sim 0.15 \times 10^{14}$ we find an error due to the approximation of only 0.46%.

Since the code is capable of evaluating the specific intensity as a function of θ and λ at any point in the shell it can be used to find values of $J_\lambda(\tau)$, $H_\lambda(\tau)$, $K_\lambda(\tau)$ and the Eddington factor, $K_\lambda(\tau)/J_\lambda(\tau)$. The Eddington factor can vary from 0.0 to 1.0 but is usually assumed to be 1/3 (the Eddington approximation, $K = 1/3\ J$) since this is the value it would have in an isotropic radiation field.

SECTION IV
RESULTS OF MODEL CALCULATIONS

The computer code used to determine the radiation field within a circumstellar dust shell is broken into three main programs (program 1, program 2, and program 3). The first is a program used to set up the integration grid and store it in the computer (usually on disk storage), the second is a program used to determine the bolometric radiation field within a dust shell and to find the temperature distribution, and the third program is used to calculate the monochromatic radiation fields for a number of wavelengths using the temperature distribution determined by the second program. The three programs must initially be run in the order given but program 1 need only be run once for each set of the geometric parameters R_*, RNR, R, τ_I, and N. Therefore it is possible to run a number of different models with the same integration grid by varying the two nongeometrical parameters T_* and ω_o .

The models that we want to consider here are characterized by the parameters in Table 1.

Table 1. Values of the seven parameters used for each of the models computed (cgs units; T_* in °K)

Model	R_*	RNR	R	τ_I	n	ω_o	T_*
I	$.202 \times 10^{13}$	$.15 \times 10^{14}$	$.75 \times 10^{15}$	5.0	1.5	0.1	6000
II	"	"	"	"	"	0.0	"
III	"	"	"	"	"	1.0	"
IV	"	"	"	"	"	0.6	"
V	"	"	"	7.0	"	0.0	"
VI	"	"	"	"	"	0.1	"
VII	"	$.202 \times 10^{13}$	$.202202 \times 10^{13}$	"	"	0.0	"
VIII	"	$.625 \times 10^{15}$	$.75 \times 10^{15}$	2.0	2.0	0.0	"
IX	"	$.15 \times 10^{14}$	"	5.0	1.3	0.1	"
X	$.8352 \times 10^{12}$	"	$.8352 \times 10^{15}$	3.97	0.0	0.8	12500

One additional model, model XI, will be described later in this section.

From Table 1 we can see that the most common values of ω_o used are 0.0 and 0.1. This is because the amount of computing time necessary to determine the radiation field is a function of ω_o. For small values of $\omega_o (\omega_o < .2)$ program 3 requires approximately six iterations to determine values of the flux, for example, converged to three significant figures, whereas, if $\omega_o = 1$ the program will need at least 15 iterations to achieve the same accuracy. Because of the high cost of models with large values of ω_o only two are

computed, models IV and X. Model III was computed for only one wavelength and therefore is not comparable in cost to models IV and X which were computed for 11 wavelength. When $\omega_o = 1.0$ we can save time by running the program for only one wavelength, λ_1, say, and then multiplying the quantities obtained for that wavelength by the factor $B(\lambda_2,T_*)/B(\lambda_1,T_*)$ to obtaine the quantities appropriate to λ_2. This is a valid procedure when $\omega_o = 1.0$ since under that condition all the radiation leaving the star must reach the surface of the shell unchanged in its spectral-energy distribution.

When program 2 is run the total outgoing bolometric flux through each shell is computed at each iteration. Since the only source of radiation is the central star, the total outgoing bolometric flux at each shell should be equal to the bolometric luminosity of the star. This is true to within 0.5% for some of the models in Table 1 and to within 4% for all the models in Table 1 except model VII. The flux (bolometric) emitted by the outer boundary of the shell in model VII is too low by 23% principally because of the very severe geometry used in model VII. This model was run as a test of the code to determine its accuracy under extreme conditions.

To determine the temperature distribution in the shell program 2 is run. The temperature distributions for the models in Table 1 are shown in Figure 3. Note that the curve for model IX is very nearly a straight line. This is due to the geometry of the shell and the fact that, as we

shall see, the radiation field in the shell is highly anisotropic. For a highly anisotropic radiation field all moments of the intensity are equal, that is $J = H = K$. Thus, $J \propto F$ and we know that $T \propto J^{1/4}$ so $T \propto F^{1/4}$. Because of conservation of flux in a spherical shell we have that $F \propto 1/r^2$; therefore, $T \propto (1/r^2)^{1/4}$ or $T \propto 1/r^{0.5}$. Therefore, for $n = 1.5$ we have from equation (6) that $\tau(r) = C_1 + C_2/r^{0.5}$, where C_1 and C_2 are constants. This means that

$$\tau(1/r^{0.5}) = C_1 + C_2\ (1/r^{0.5})$$

and, therefore we can see that τ will be a linear relation of T.

The temperatures of the dust grains as mentioned in Section I are consistent with the assumption that they are carbon grains where the temperature is below about 2100°K and consistent with the assumption that they are refractory silicates for temperatures less than about 1500°K. Note that the spread in temperatures at $\tau = 0$ is small even though some of the models have very different physical parameters.

Program 3 is run to determine a variety of quantities for the cloud. These quantities are: $I(\lambda,\tau,\theta)$, $J(\lambda,\tau)$, $K(\lambda,\tau)/J(\lambda,\tau)$, and $F(\lambda,\tau)$. Figures 4 and 5 show some representative values of these quantities (computed for model IX). The conversion of visual to infrared radiation can be seen on Figure 4 by following the relative intensities of a few wavelengths from $\tau = 7$ to $\tau = 0$. Figure 5

also shows this by way of the graphs for J and F. The graphs for K/J show that the radiation field is generally anisotropic although at depth the infrared radiation field does approach the Eddengton approximation, K/J = 1/3. Thus, the use by Huang and Apruzese of the Eddington approximation can be expected to decrease the accuracy of their results significantly.

In Figure 6 the run of temperature with optical depth is shown for two models calculated with this code and for two models calculated by Huang (1971). The two models calculated with this code are models VIII and XI. Model XI has the following parameters: $\tau_I = 2.32$, $R_* = .202 \times 10^{13}$ cm, RNR = $.609 \times 10^{15}$ cm, R = $.75 \times 10^{15}$ cm, n = 2.0 and $T_* = 6000°K$. For optical depths larger than about 2/3 the curves for models VIII and XI are very similar the curves for Huang's corresponding models. From optical depth 2/3 to 0 the curves for models VIII and XI drop off much more rapidly than Huang's curves. This is just what we would expect to happen due to the erroneous value of the Eddington factor used by Huang for the outer part of the cloud.

Figure 7 shows the spectral-energy distribution for HD 45677 as given by Swings and Allen (1971) and Low et al. (1970). On the same graph the spectral-energy distribution for model X is also plotted. Model X is based on a set of parameters derived by Apruzese (1974) for HD 45677. He determined these parameters by fitting the observations in the visual since his model is not capable of directly

fitting the infrared observations (actually his model does use the infrared data in that he attempts to make the total infrared emission calculated by his model equal to the total infrared emission given by the observations). The graphs show that his parameters do give a very good fit in the visual region and that the total emission in the infrared predicted by his parameters is approximately correct; however, his parameters do not give a good fit to the actual infrared spectral-energy distribution. A different set of parameters could be found that would fit both the visual and the infrared regions.

Figures 8 and 9 show the spectral energy distributions for a number of the models listed in Table 1. On Figure 8 the graphs for models II, V, VIII and X are shown. The curve for model VI would fall between those for models II and V. We can see the effect of changing the various model parameters by studying these curves.

The curves for models II and V show that increasing the total optical depth of the shell causes the peak of the distribution to move toward the red (Figure 3 shows that at the same time the temperature of the inner part of the shell goes up) and causes the amount of visual radiation filtering through to decrease by a large amount.

Models VIII and X show, as we would expect, that when the optical depth of the shell is decreased by a large amount the central star causes the distribution to peak in the visual.

Figure 9 shows the spectral-energy distributions for models I, IV, IX and the means of the observations of R Mon due to Mendoza (1966, 1968), Low and Smith (1966) and Low et al. (1970), where vertical bars show the amount of variability from those means. The vertical error bars on the observations at 20 and 22μ indicate the root-mean-square error of a single observation, approximately 20%.

The U through M values plotted are intensities calculated from Mendoza's observations (corrected for interstellar extinction), using Johnson's (1966) calibration of the UBVRIJKLM system. The interstellar extinction correction was made, assuming that R Monocerotis is located in NGC 2264, and using the following adopted data for that cluster and hence R Monocerotis: $E_{B-V} = 0.06$ (Strom et al. 1971) and a reddening curve of the NGC 2244 type with $R = 5.4$ (Johnson, 1968).

Using these values we have $A_V = 0.324$, and from the reddening curve we obtain the extinction in magnitudes, ΔM, for each of the observed colors (see Table 2).

The root-mean-square errors of a single observation are shown for the 20μ and the 22μ observations in Figure 9, but for all the other bands the root-mean-square errors of a single observation are negligible, considering the intrinsic variability of the object. The largest such error is for the M band, and it amounts to less than 0.1 magnitudes.

Table 2. Interstellar extinction in magnitudes, Δm, for R Monocerotis in each of the colors observed

Band	Δm
U	0.424
B	0.383
V	0.324
R	0.277
I	0.224
J	0.189
K	0.141
L	0.094
M	0.083

The curve for model IV shows that a large increase in the value of ω_o causes the peak of the distribution to narrow and move toward the blue, it also shows that the direct contribution of the star in the visual increases greatly. The curves for models I and IX show that a small increase in the index n causes the peak of the distribution to move toward the blue, while the ends of the curve in the visual and far infrared drop.

Model I is the best fit to the observations of R Mon but it looks as though Model IX with a slightly larger ω_o would fit somewhat better.

The following discussion pertains to the development of the model for R Mon.

The spectral class of R Monocerotis, roughly G (Joy, 1945), and luminosity of 870 $L_\odot$ (Low and Smith, 1966) lead to the values of T_* and R_* chosen for these values since $4\pi R_* \sigma T_*^4 \sim 870 L_\odot$. The value for τ_I was determined from a cursory examination of the observations in the following manner. We have the ratio of the visual flux, F_V, to the bolometric flux, F_B, for R Monocerotis; namely, $F_V/F_B \sim .006$ (Low and Smith, 1966). From this and the relation $\tau_I = \ell n(F_V/F_B)$ we obtain for $\tau(R_I)$; $\tau_I \sim 5$.

It should be noted that this method gives only a lower limit to τ_I, since we cannot say what portion of F_V is actually coherently scattered radiation. Thus, ω_o and τ_I cannot be determined separately with any ease. The values of ω_o, R_I, R and n used were just rough initial approximations.

We must consider the following observational data for R Monocerotis: (a) the spectrum does not show selective absorption (Joy, 1945), (b) strong variable optical polarization exists indicating scattering by large grains (Zellner, 1970), and (c) irregular light variations occur of several magnitudes (Joy, 1945; Mendoza, 1966, 1968; Low et al. 1970). In addition we have the UBVRIJKLMQ observations of Mendoza, Low and Smith, and Low et al. mentioned previously.

Points (a) and (b) above are consistent with the assumption that the cloud is made up of solid particles which act as grey absorbers and emitters. For a period of

variation of the polarization which is fairly short, the assumption that the particles are randomly oriented should be reasonable. Because of the variability mentioned in point (c), those observations in several colors, which were made on the same day are of the greatest interest, and where such observations are lacking, we are forced to compare the computed fluxes to mean observed fluxes.

Using the parameters from Case I given by

$$\tau_I = 5 ,$$
$$R_I = .15 \times 10^{14} \text{ cm} ,$$
$$R = .75 \times 10^{15} \text{ cm} ,$$
$$n = 1.5 ,$$

and assuming the particles to have the density of carbon or silicon dioxide; that is, $\rho_p \sim 2.0$, we have from equation (25) for the mass of the cloud.

$$M = 13dM_\odot .$$

This gives us for particles about twenty microns in diameter a cloud mass of about $10^{-2}M_\odot$.

The set of parameters for Case I also gives us for equation (24) the following form:

$$\rho(r) = (1.5 \times 10^9) \frac{d}{r^{1.5}} .$$

If $d = 20\mu$ and r ranges from 10^{13} to 10^{15} cm, then $\rho(r)$ will range from approximately 10^{-13} to 10^{-16} grams/cm^3.

In summary, the best fit to the observations was obtained by a model with the following parameters:

$$R_I = .15 \times 10^{14} \text{ cm } (\sim 1\text{Au}) ,$$

$R = .75 \times 10^{15}$ cm (~50 Au) ,

$\tau_I = 5$,

$\omega_o = 0.1$,

$n = 1.5$,

$M \sim 10^{-2} M_\odot$

$10^{-16} < \rho(r) < 10^{-13}$ gm/cm^3 ,

$225°K < T < 2{,}100°K$.

Figure 1. Radiation is shown falling on point 1 at distance r from the central star. It is incident there at an angle θ_1 after being emitted from point 2 at an angle θ_e. Part of this emitted radiation is radiation from point 3 which was incident on point 2 at an angle θ_2, and scattered through an angle α. Point 2 is a distance r_e from the central star and a distance s(t) from point 1. Analogous triangles, with vertices at the star, point 1 and any point on the line directed from point 1, at the angle θ_1, can be constructed.

Note that the angle θ_1 is designated simply θ in the text.

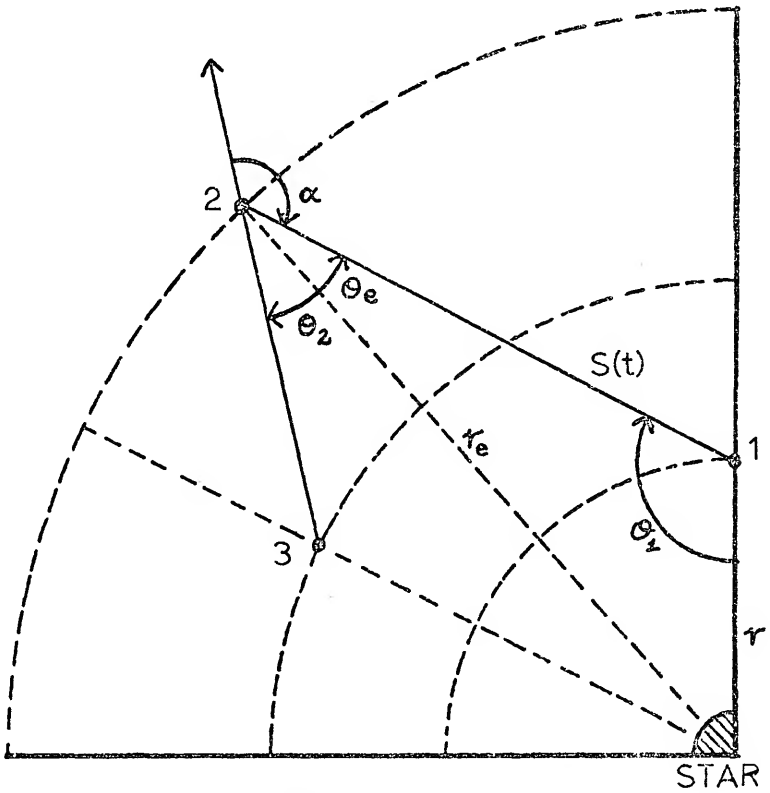
2
α
θe
θ2
S(t)
re
1
θ1
3
r
STAR

Figure 2. A schematic diagram of the integration grid for the case when N = 4. Four lines of sight are shown to indicate the manner in which the boundary conditions at r_1 and r_n are handled. The filled circles on the lines represent the initial grid of intersection points. The tick marks on the lines represent the points found at equal intervals of τ by an iterative technique. The open circles represent the Gauss-Legendre points for a three point quadrature formula.

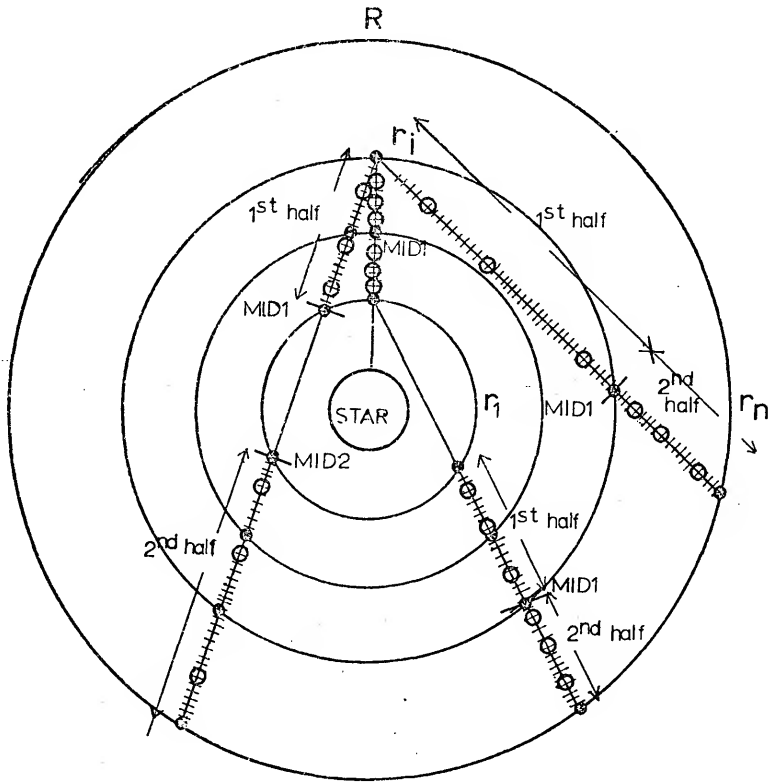
R
r_i
1st half
MID1
1st half
MID1
2nd half
r_n
STAR
r_1
MID1
MID2
1st half
2nd half
MID1
2nd half

Figure 3. Temperature in degrees Kelvin vs. optical depth. The model number is shown for each curve (see Table 1 for model parameters).

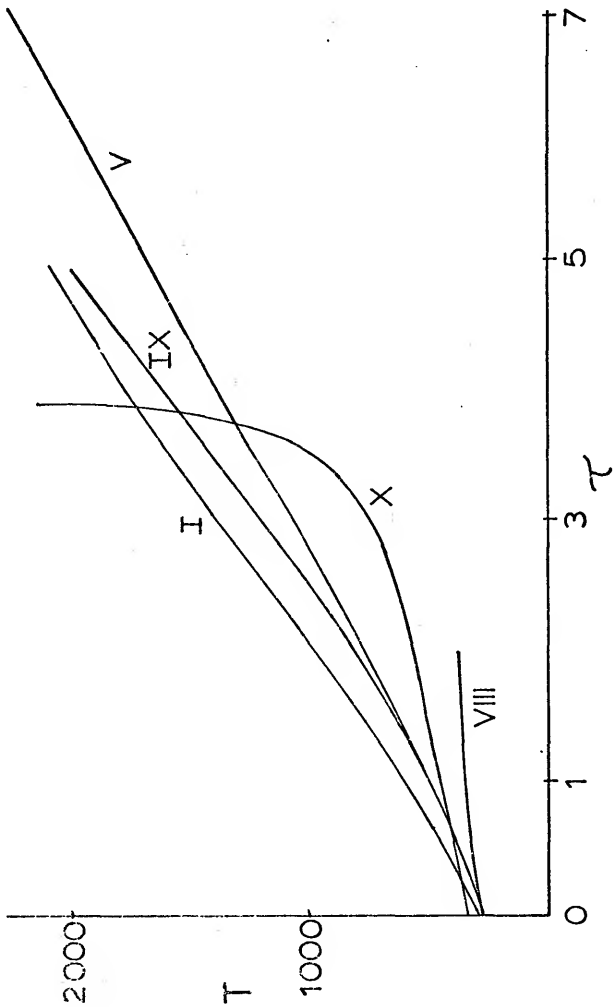
V
IX
I
X
VIII
2000
1000
T
0
1
3
5
7
τ

Figure 4. Log [$I(\lambda,\theta,\tau)$] vs. θ for model IX. The angle θ is in radians. The three panels from top to bottom are for τ = 7.0; 3.68; 0.0. The curve are labeled with letters designating their respective wavelengths on the UBVRIJKLMNQ system. Note that in the case for τ = 7.0 the star is not considered a point.

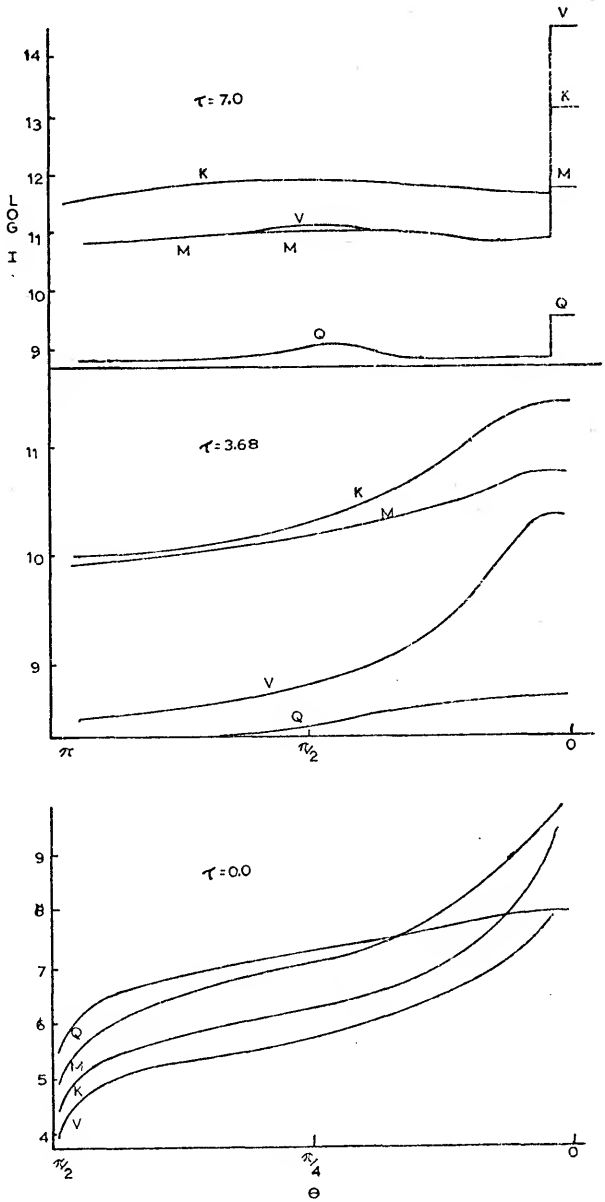
LOG I
14
13
12
11
10
9
τ = 7.0
K
V
M
M
M
V
K
M
Q
Q
11
10
9
τ = 3.68
K
M
V
Q
π
π/2
0
9
8
7
6
5
4
τ = 0.0
Q
M
K
V
π/2
π/4
0
θ

Figure 5. Log $[J(\lambda,\tau)]$, $K(\lambda,\tau)/J(\lambda,\tau)$, and Log $[F(\lambda,\tau)]$ vs. τ for model IX. The curves are labeled with letters designating their respective wavelengths on the UBVRIJKLMNQ system.

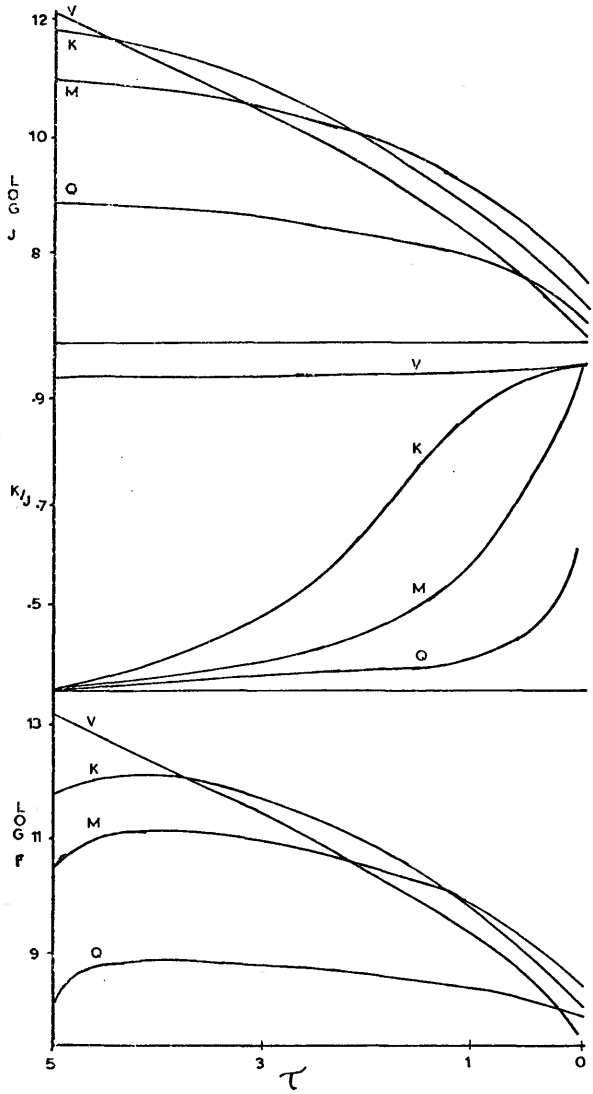
12
10
8
LOG J
V
K
M
O
.9
.7
.5
K/J
V
K
M
O
13
11
9
LOG F
V
K
M
O
5
3
1
0
τ

Figure 6. Normalized temperature, T/T_o, vs. τ . Here T_o is the temperature at optical depth zero. The upper pair of solid curves represent the temperature distributions for models VIII and XI (see Table 1 for model parameters for model VIII and the text on page 60 for model parameters for model XI) where the curve labeled 2.3 is for model XI and the one labeled 2.0 is for model VIII. The numbers labeling the curves give the maximum optical depth, τ_I, for that model. The lower pair of curves represent the temperature distributions for two models calculated by Huang (1971). The lower curve labeled 2.0 is for a model with parameters identical to model VIII and the curve labeled 2.4 is for a model with parameters very similar to model XI. The dotted curve is the lower curve labeled 2.0 scaled to coincide with the curve for model VIII at $\tau = 2.0$ (the two curves are superimposed for optical depths larger than about 2/3).

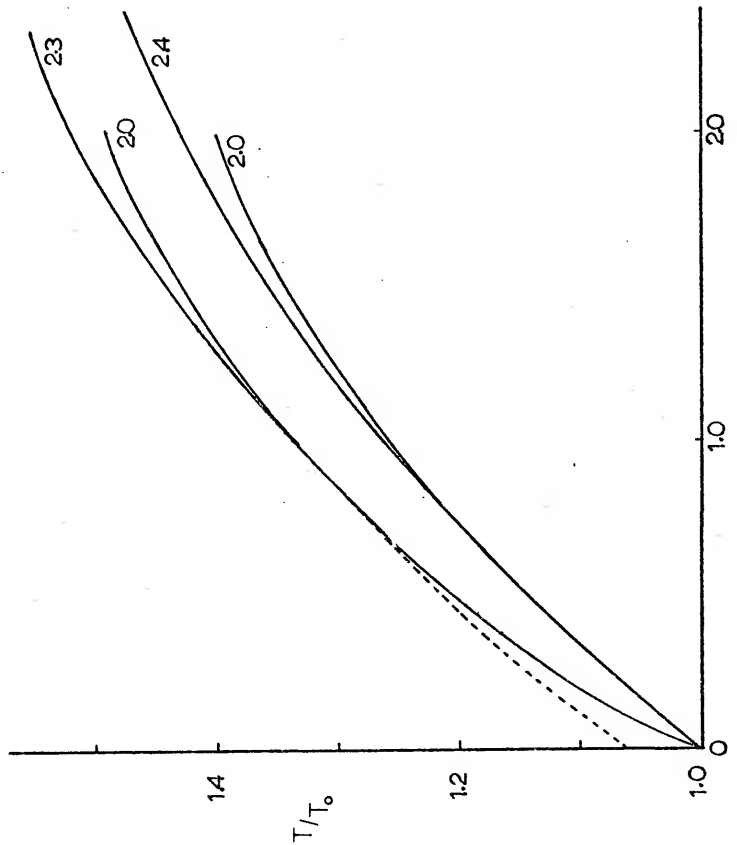
23
20
24
2.0
1.4
1.2
1.0
T/T₀
0
1.0
2.0
τ

Figure 7. The spectral-energy distribution for HD 45677 (curve A) and the spectral-energy distribution found for model X (curve B). Note that, λF_λ vs. Log (λ) is plotted and that therefore the area under a segment of the curve is equal to the energy in that wavelength interval. The curves are normalized to the peak of model X's distribution.

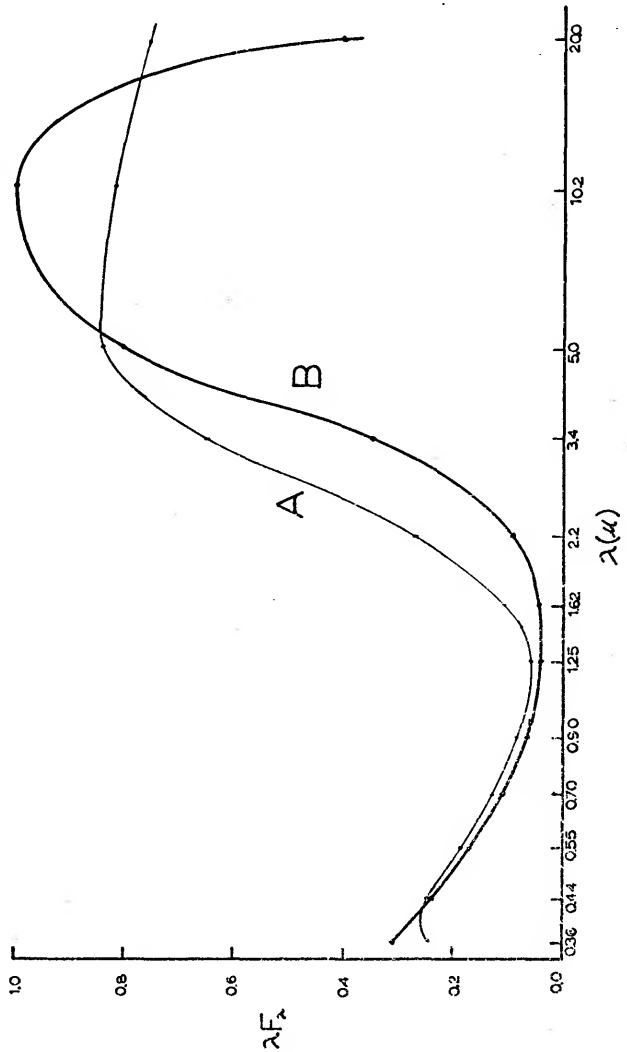
1.0
0.8
0.6
0.4
0.2
0.0
λF_λ
0.36
0.44
0.55
0.70
0.90
1.25
1.62
2.2
3.4
5.0
10.2
20.0
λ(μ)
A
B

Figure 8. $F(\lambda)$ vs. λ for models II, V, VIII, and X (see Table 1 for model parameters).

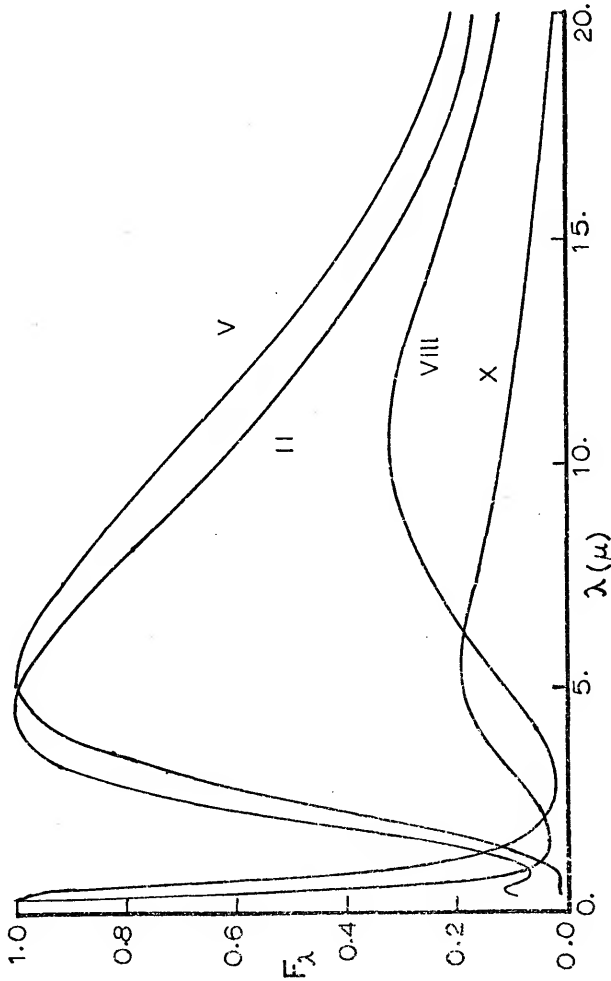
1.0
0.8
0.6
F_λ
0.4
0.2
0.0
0.
5.
10.
15.
20.
$\lambda(\mu)$
V
II
VIII
X

Figure 9. $F(\lambda)$ vs. λ for a 850°K Blackbody curve, the observed spectral-energy distribution for R Mon (vertical bars) and the spectral-energy distributions for models I, IV, and IX. The curve for model IX is dashed for clarity. The vertical bars at 20 and 22 μ are error bars whereas the others indicate the range of variability of the object.

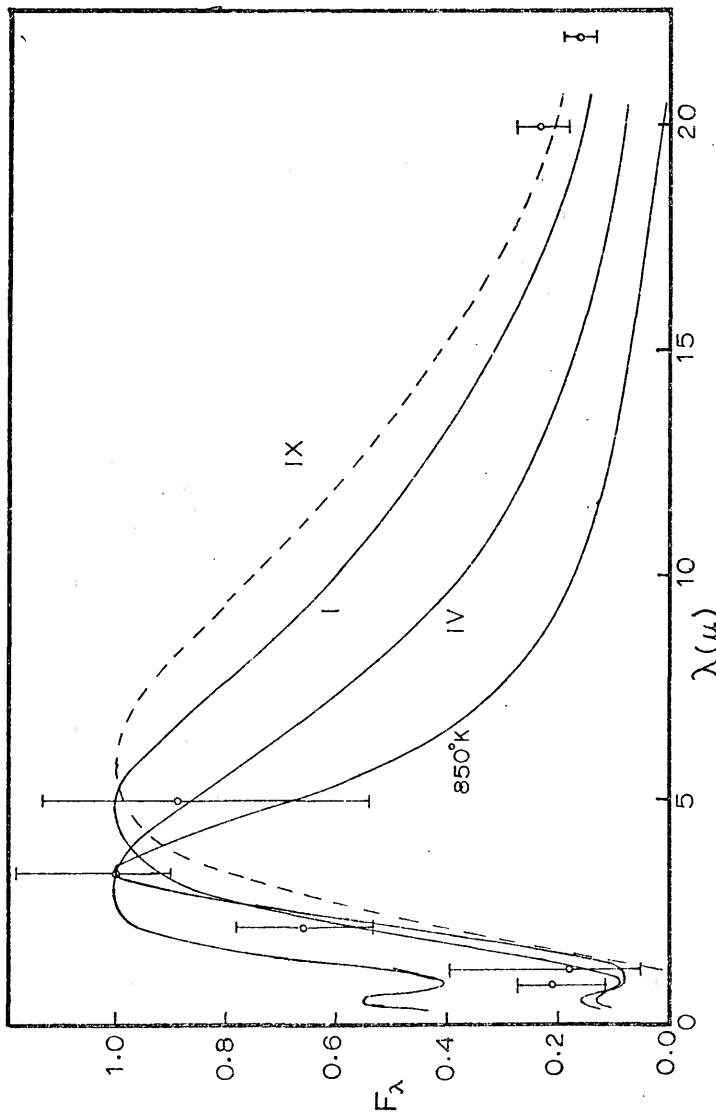
IX
I
IV
850°K
1.0
0.8
0.6
0.4
0.2
0.0
F_λ
0
5
10
15
20
$\lambda(\mu)$

Figure 10. Mendoza's observations of R Monocerotis out to 0.9 microns corrected for interstellar extinction and normalized to the mean of his 3.4 micron observations. Each curve represents the observations of a different night.

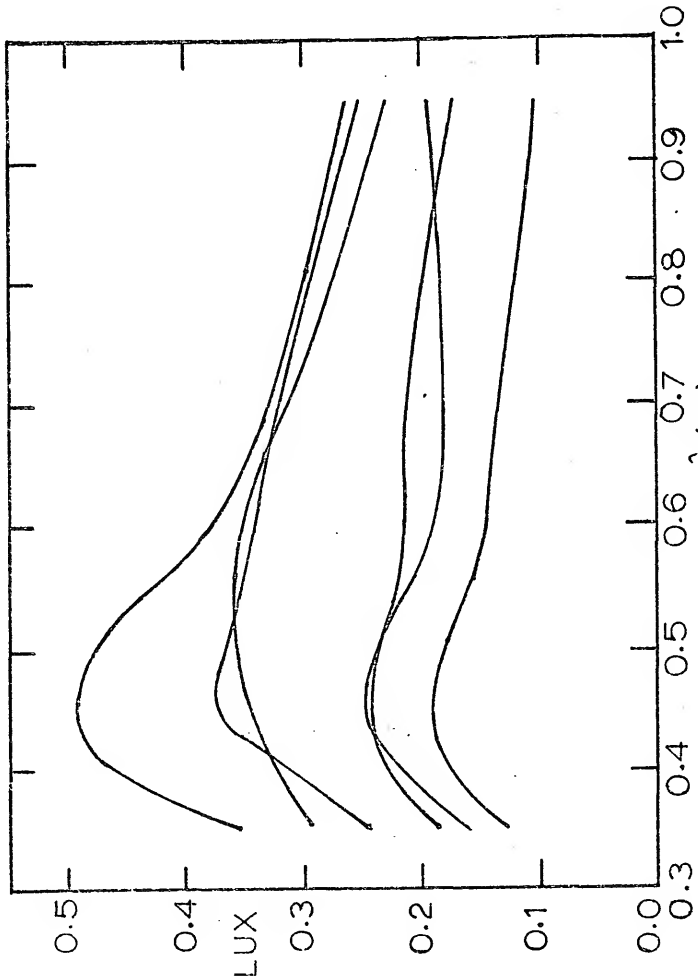
FLUX
0.5
0.4
0.3
0.2
0.1
0.0
0.3
0.4
0.5
0.6
0.7
0.8
0.9
1.0
λ(μ)

LIST OF REFERENCES

Ackermann, G., Fugmann, F., Hermann, W., and Voelcker, K. 1968, Z. Ap., 69, 130.

_____. 1970, Astron, Ap., 8, 315.

Anderson, L., and Kuhi, L.V. 1969, Non-Periodic Phenomena in Variable Stars, ed. L. Detre (Dordrecht-Holland: D. Reidel Publishing Co.), p. 93.

Apruzese, J.P. 1974, Ap. J., 188, 539.

Breger, M. 1972, Ap. J., 171, 539.

Breger, M., and Dyck, H.M. 1972, Ap. J., 175, 127.

Capps, R.W., and Dyck, H.M. 1972, Ap. J., 175, 693.

Chandrasekhar, S. 1934, M.N.R.A.S., 94, 444.

Chavira, E. 1967, Bol. Obs. Tonantzintla y Tacubaya, 4, 29.

Cohen, M. 1973a, M.N.R.A.S., 161, 85.

_____. 1973b, ibid., p. 97.

_____. 1973c, ibid., p. 105.

Gilman, R.C. 1969, Ap. J., 155, L185.

Grasdalen, G.L., and Gaustad, J.E. 1971, A.J., 76, 231.

Hayashi, C. 1966, Ann. Rev. Astr. and Ap., 4, 171.

Herbig, G.H. 1960.

_____. 1968, Ap.J., 152, 439.

_____. 1970, ibid, 162, 557.

Hetzler, C. 1937, ibid., 86, 509.

Hildebrand, F.B. 1956, Introduction to Numerical Analysis (New York/Toronto/London: McGraw-Hill), p. 49.

Huang, Su-Shu 1969a, Ap. J., 157, 835.

_____. 1969b, ibid., 157, 843.

Huang, Su-Shu, 1971, ibid., 164, 91.

Hummer, D.G., and Rybicki, G.B. 1971, M.N.R.A.S., 152, 1.

Hyland, A.R., Becklin, E.E., Neugebauer, G., and Wallersten, G. 1969, Ap. J., 158, 619.

Johnson, H.L. 1966, Ann. Rev. Astr. and Ap., 4, 193.

_____. 1968, Nebulae and Interstellar Matter, ed. B.M. Middlehurst and L.H. Aller (Chicago: University of Chicago Press), p. 202.

Joy, A.H. 1945, Ap. J., 102, 168.

Krishna Swamy, K.S. 1970, Ap. and Space Science, 9, 123.

Kukarkin, B.V., Kholopov, P.N., Efremov, Yu, N., Kukarkina, N.P., Kurochkin, N.E. Medvedea, G.I., Perova, N.B., Federovich, M.S., and Frolov, M.S. 1969, General Catalogue of Variable Stars, Third Edition (Moscow).

Larson, R.B. 1969a, M.N.R.A.S., 145, 271.

_____. 1969b, ibid., 145, 297.

Low, F.J., and Smith, B.J. 1966, Nature, 212, 675.

_____. 1970, Semi-Ann. Tech. Rep. Contract No. F 19628-70-C-0046 Project No. 5130 (ARPA).

Low, F.J., Johnson, H.L., Kleinmann, D.E., Latham, A.S., and Geisel, S.L. 1970, Ap. J., 160, 531.

Mendoza, V.E.E. 1966, Ap. J., 143, 1010.

_____. 1968, Ap. J., 151, 977.

Mihalas, D. 1970, Stellar Atmospheres (San Francisco: W.H. Freeman and Company), p. 5.

Mullen, J. 1974 (Private Communication).

Neugebauer, G., Becklin, E., and Hyland, A.R. 1971, Ann. Rev. Astr. and Ap., 9, 67.

Neugebauer, G., and Leighton, R.B. 1969, Two-Micron Sky Survey - a Preliminary Catalog (NASA SP-3047).

Poveda, A. 1965a, Bol. Obs. Tonantzintla y Tacubaya, 4, 15.

_____. 1965b, ibid., 26, 15.

_____. 1965c, ibid., 26, 22.

Prentice, A.F.R., and terHaar, D. 1971, M.N.R.A.S., 151, 177.

Serkowski, K. 1971, Proceedings of the Conference on Late-Type Stars, ed. G.W. Lockwood and H.M. Dyck (Kitt Peak Contr. No. 554), p. 107.

Stein, W. 1966, Ap. J., 145, 101.

Strom, K.M., Strom, S.E., and Yost, J. 1971, Ap. J., 165, 479.

Strom, S.E. 1972, PASP, 84, 745.

Strom, S.E., Strom, K.M., Brooke, A.L., Breger, J., and Yost, J. 1972, Ap. J., 171, 267.

Swings, J.P., and Allen, D.A. 1971, Ap. J., 167, L41.

Walker, M.F. 1969, Non-Periodic Phenomena in Variable Stars, ed. L. Detre (Dordrecht-Holland: Reidel Publishing Co.), p. 103.

Walker, M.F. 1972, Ap. J., 175, 89.

Woolf, N.J., Stein, W.A., and Strittmatter, P.A. 1970, Astron. Ap., 9, 252.

Zellner, B. 1970, A.J., 75, 182.

Zellner, B.H., and Serkowski, K. 1972, PASP, 84, 619.

BIOGRAPHICAL SKETCH

Christopher Alvin Harvel was born on December 7, 1944 in Columbia, South Carolina. He attended public schools in North Carolina, California, New Jersey, and Virginia, graduating from McLean High School in McLean Virginia in 1963. Four years later, in 1967, he received his Bachelor of Science degree with a major in Astronomy from Georgetown University in Washington, D.C. and started graduate school at the University of South Florida.

In December of 1968 he was drafted into the United States Army and in December of 1969 he began a one-year tour of duty in the Republic of South Vietnam.

At the end of his military service in December of 1970, he returned to the University of South Florida and received a Master of Arts degree in Astronomy in 1972. In that same year he started graduate school at the University of Florida where receipt of the Ph.D. degree should occur in August, 1974.

I certify that I have read this study and that in my opinion it conforms to acceptable standards of scholarly presentation and is fully adequate, in scope and quality, as a dissertation for the degree of Doctor of Philosophy.

Frank Bradshaw Wood

Frank Bradshaw Wood, Chairman
Professor of Physics and
Astronomy

I certify that I have read this study and that in my opinion it conforms to acceptable standards of scholarly presentation and is fully adequate, in scope and quality, as a dissertation for the degree of Doctor of Philosophy.

Sabatino Sofia

Sabatino S. Sofia
Professor of Astronomy
University of South Florida

I certify that I have read this study and that in my opinion it conforms to acceptable standards of scholarly presentation and is fully adequate, in scope and quality, as a dissertation for the degree of Doctor of Philosophy.

Kwan Yu Chen

Kwan-Yu Chen
Associate Professor of Physics
and Astronomy

I certify that I have read this study and that in my opinion it conforms to acceptable standards of scholarly presentation and is fully adequate, in scope and quality, as a dissertation for the degree of Doctor of Philosophy.

Howard L. Cohen
Associate Professor of Physical Sciences and Astronomy

I certify that I have read this study and that in my opinion it conforms to acceptable standards of scholarly presentation and is fully adequate, in scope and quality, as a dissertation for the degree of Doctor of Philosophy.

James W. Dufty
Assistant Professor of Physics

This dissertation was submitted to the Graduate Faculty of the Department of Physics and Astronomy in the College of Arts and Sciences and to the Graduate Council, and was accepted as partial fulfillment of the requirements for the degree of Doctor of Philosophy.

August, 1974

Dean, Graduate School